Zurich, 8 February 2017

Dear Prof. Markus Weiler,

Please find attached the revised version of our manuscript entitled “A lab in the field: High-frequency analysis of water quality and stable isotopes in streamwater and precipitation” (hess-2016-585).

We addressed all issues raised by the reviewers (our detailed responses to the reviewers are already posted). In particular, following the reviewer’s suggestion, we have compressed section 5, for instance by merging sections 5.3 and 5.4 into one section. We further added sub-headings to section 5.2 to better structure this part of the revised manuscript and to make it easier for the reader to follow the train of thought.

Further, we included more references to previous studies to link our research to other potential approaches. Among others, we reference a review paper by Rode et al. (2016) that presents a comprehensive overview of the most recent applications of high-frequency measurements of isotopes and solutes in hydrology. Unfortunately, we did not find any oceanography studies where high-frequency isotope measurements are used (or could be used), however, we hope that our paper may arouse interest within the ocean research community.

We highly appreciated the thoughtful comments of you and the two reviewers, which helped to improve our manuscript. We believe that the revised version of our manuscript illustrates more clearly the novelty of our analysis system and describes in more detail the application of high-frequency measurements of stable water isotopes and major ions in catchment studies.

Thank you for considering our revised manuscript.

Best regards,

Jana von Freyberg, Bjørn Studer and James W. Kirchner

A lab in the field: High-frequency analysis of water quality and stable isotopes in streamwater and precipitation

Jana von Freyberg[1,2], Bjørn Studer[1], James W. Kirchner[1, 2]

[1] Department of Environmental Systems Science, ETH Zurich, Zurich, Switzerland

[2] Swiss Federal Research Institute WSL, Birmensdorf, Switzerland

Correspondence to: Jana von Freyberg (jana.vonfreyberg@usys.ethz.ch)

Abstract. High-frequency measurements of solutes and isotopes (^{18}O and ^{2}H) in rainfall and streamflow can shed important light on catchment flow pathways and travel times, but the workload and sample storage artifacts involved in collecting, transporting, and analyzing thousands of bottled samples severely constrain catchment studies where conventional sampling methods are employed. However, recent developments towards more compact and robust analyzers have now made it possible to measure chemistry and water isotopes in the field at sub-hourly frequencies over extended periods. Here we present laboratory and field tests of a membrane-vaporization continuous water sampler coupled to a cavity ring-down spectrometer for real-time measurements of $\delta^{18}O$ and $\delta^{2}H$, combined with a dual-channel ion chromatograph (IC) for synchronous analysis of major cations and anions. The precision of the isotope analyzer was typically better than 0.03 ‰ for $\delta^{18}O$ and 0.17 ‰ for $\delta^{2}H$, for 10 min average readings taken at intervals of 30 min. Carryover effects were less than 1.2 % between isotopically contrasting water samples for 30 min sampling intervals, and instrument drift could be corrected through periodic analysis of secondary reference standards. The precision of the ion chromatograph was typically ~0.1-1 ppm or better, with relative standard deviations of ~1% or better for most major ions in streamwater, sufficient to detect subtle biogeochemical signals in catchment runoff.

We ~~tested~~ installed the coupled isotope analyzer / IC system in an uninsulated hut next to a stream of a small catchment and ~~under field conditions by~~ analyz~~ed~~ing streamwater and precipitation samples every 30 min over 28 days ~~in a small catchment~~. These high-frequency measurements facilitated a detailed comparison of event-water fractions via end-member mixing analysis with both chemical and isotope tracers. For two events with relatively dry antecedent moisture conditions, event-water fractions were <21 ~~0~~% based on isotope tracers, but were significantly overestimated (40 ~~39~~% to 82 ~~3~~%) by the chemical tracers. These observations, coupled with the storm-to-storm patterns in precipitation isotope inputs and the associated streamwater isotope response, led to a conceptual hypothesis for runoff generation in the catchment. Under this hypothesis, the pre-event water that is mobilized by precipitation events may, depending on antecedent moisture conditions, be significantly shallower, younger, and less mineralized than the deeper, older water that feeds base flow and thus defines the "pre-event" end-member used in hydrograph separation. This proof-of-concept study illustrates the potential advantages of capturing isotopic and hydrochemical behavior at high frequency over extended periods that span multiple hydrologic events.

1. Introduction

Environmental tracers are widely used in hydrology to investigate recharge processes, subsurface flow mechanisms and streamflow components (Leibundgut and Seibert, 2011). The most common environmental tracers are the naturally occurring stable water isotopes ^{18}O and ^{2}H (Klaus and McDonnell, 2013). Solutes such

as dissolved organic compounds, nutrients, and major ions are also widely used, together with stable isotopes, as indicators of flowpaths and biogeochemical reactions (e.g., McGlynn and McDonnell, 2003; Vitvar and Balderer, 1997; Weiler et al., 1999). Environmental tracer studies typically involve manual or automated sample collection, followed by transport, storage, and subsequent laboratory analysis. The time and effort involved in sample handling are often a major constraint limiting the frequency and duration of sampling, and thus the scope of tracer studies. While various automated, in-situ analyzers for certain solutes and nutrients are becoming standard tools in environmental monitoring studies (e.g., Bende-Michl and Hairsine, 2010; Rode et al., 2016b), high-frequency analyses of isotopes and major ions over longer time periods remain challenging.

To date, isotope studies have maintained high sampling frequencies only during a few storm events (e.g., Berman et al., 2009; Lyon et al., 2008; Pangle et al., 2013), with the result that only limited ranges of catchment behavior have been explored. Long-term catchment studies capture a wider range of hydrologic events, but generally collect water samples at only weekly or monthly intervals for subsequent laboratory analysis (e.g., Buso et al., 2000; Darling and Bowes, 2016; Jasechko et al., 2016, Neal et al., 2011), making higher-frequency behaviors unobservable. As pointed out by Kirchner et al. (2004), sampling at intervals much longer ~~much smaller~~ than the hydrological response times of a catchment may result in significant losses of information. For instance, sub-daily sampling is required to capture diurnal fluctuations in streamwater hydrochemistry, which reflect evapotranspiration effects or in-stream biological activity (e.g., Aubert and Breuer, 2016; Hayashi et al., 2012). ~~Thus, high-frequency sampling can help to determine ecological effects or to identify biogeochemical hot spots and hot moments, which are characterized by disproportionately high reaction rates (e.g., McClain et al., 2003; Vidon et al., 2010).~~ In order to differentiate hydrological and biogeochemical catchment processes related to different water ages and flow pathways, long-term monitoring has to be complemented by additional high-frequency hydrochemical and isotope measurements. So far, only a few long-term studies have sampled streamwater at daily or sub-daily intervals for on-site measurements or subsequent analysis in the laboratory, such as at Plynlimon, Wales (Neal et al., 2012), at the Kervidy-Naizin catchment in western France (Aubert et al., 2013) or at the Selke river in Germany (Rode et al., 2016a). Such studies have yielded fundamental insights into catchment hydrological behaviour, not only at a wide range of temporal scales but also under varying hydro-climatic conditions (e.g., Benettin et al., 2015; Halliday et al., 2013; Harman, 2015; Kirchner and Neal, 2013; Riml and Worman, 2015).

The recent development of compact and robust isotope analyzers has fostered initial attempts to continuously measure $\delta^{18}O$ and $\delta^{2}H$ in streamwater or precipitation directly in the field. The only previous field-based isotope monitoring of 4 contiguous weeks was carried out by Berman et al. (2009) with a customized liquid water isotope analyzer based on off-axis integrated cavity output spectroscopy (OA-ICOS; Los Gatos Research, Mountain View, CA, USA), which measured $\delta^{18}O$ and $\delta^{2}H$ in 90 samples per day. As the system was based on repeated injections of samples into a vaporizer, daily maintenance (i.e., injection septa change, filter cleaning) was required to keep it running. An alternative approach uses a semi-permeable membrane to generate water vapor from a continuous sample throughflow, which is then transferred to a wavelength scanned – Cavity Ring-Down Spectrometer (CRDS) (e.g., Herbstritt et al., 2012). Munksgaard et al. (2011) developed such a custom-made diffusion sampler and attached it to a CRDS (Picarro Inc., Santa Clara, CA, USA) that was used to

78 measure $\delta^{18}O$ and $\delta^{2}H$ in precipitation at frequencies of up to 30s over a 15day period (Munksgaard et al.,
79 2012), as well as to monitor the isotopic response at 1 min resolution in streamflow during a storm event
80 (Tweed et al., 2016).
81
82 A similar diffusion sampling system has recently become commercially available (Continuous Water Sampler
83 Module, or CWS; Picarro Inc., Santa Clara, CA, USA), which allows for quasi-continuous measurements of
84 $\delta^{18}O$ and $\delta^{2}H$ in liquid water samples when coupled to a CRDS analyzer. Here we present initial laboratory and
85 field verification experiments with this device, which we have combined with a dual-channel ion chromatograph
86 (IC; Metrohm AG, Herisau, Switzerland) for real-time analysis of major cations and anions. Laboratory
87 experiments quantifying the precision and sample carryover memory effects of this system are presented in
88 Section 3 below. Section 4 illustrates the ~~practical application~~performance of the system in the field using a 28-
89 day deployment at a small catchment in Switzerland. Section 5 quantifies the fractions of event water that
90 contributed to the flood hydrograph in eight ~~major precipitation~~ storm events, illustrating one potential
91 application of high-frequency ~~isotope tracer~~ measurements of isotopes and major ions.

92 **2. Methodology**

93 **2.1 Isotope analysis and ion chromatography**

94 For the analysis of the stable water isotopes ^{18}O and ^{2}H, the Continuous Water Sampler module (CWS; Picarro
95 Inc., Santa Clara, CA, USA) was coupled to a Wavelength Scanned-Cavity Ring-Down Spectrometer (WS-
96 CRDS; model L2130-*i*, Picarro Inc., Santa Clara, CA, USA). In the CWS, the water sample flows at a rate of
97 ~1mL min^{-1} through an expanded polytetrafluouroethylene (ePTFE) membrane tube. This tube is mounted in a
98 stainless steel chamber that is supplied with dry air to facilitate the steady diffusion of a small fraction of the
99 through-flowing water as vapor through the membrane. Through the continuous flow of dry air over the outer
100 surface of the membrane, the vapor is carried directly to the CRDS for isotope analysis. To minimize
101 temperature-induced fractionation effects, the instrument keeps the temperatures of the membrane chamber and
102 the inflowing water constant at (± 1 standard deviation) 45±0.1°C and 15±0.1°C, respectively. A solenoid
103 diaphragm pump situated upstream of the membrane cartridge draws water samples from the sample container
104 and pushes them through the membrane tube at a flow rate of approximately 1 mL min^{-1}. As we show in
105 Section 3.1 below, preliminary tests showed that this pump is not sufficient for our purposes, so we substituted a
106 programmable high-precision dosing unit (800 Dosino, Metrohm AG, Herisau, Switzerland) in its place.
107
108 Isotopic abundances are reported through the δ notation relative to the VSMOW-SLAP standards. ~~We used~~ For
109 the laboratory experiments, we used the factory calibration of the isotope analysis system, because only relative
110 isotope values are needed for quantifying precision, drift, and carryover, and thus the absolute isotope values are
111 unimportant. For the field experiment, however, we periodically measured two internal isotope standards (Fiji
112 and Evian bottled water), which were calibrated by a Picarro L2130-*i* CRDS at the isotope laboratory of the
113 University of Freiburg (Germany) to primary reference materials (IAEA standards SLAP, VSMOW, GISP;
114 instrument precision 0.16 ‰ ($\delta^{18}O$) and 0.6 ‰ ($\delta^{2}H$)).
115

Major ions in liquid water samples, i.e. Na^+, K^+, NH_4^+, Ca^{2+}, Mg^{2+}, F^-, Cl^-, NO_3^-, SO_4^{2-}, PO_4^{3-}, were analyzed with an ion chromatograph (IC; model 940 Professional IC Vario, Metrohm AG, Herisau, Switzerland) with a two-column configuration (Anions: Metrosep A Supp 5 – 250/4.0, Cations: Metrosep c 6 – 250/4.0). Continuous operation of the instrument was possible due to fully automated eluent generation (941 Eluent Production Module). To generate the full ion chromatograms of both anions and cations, approximately 28 min were required; thus the sampling interval of the combined analysis system was fixed at 30 min.

2.2 Sample collection and distribution

The water samples were distributed between the analyzers with high-precision dosing units (800 Dosino, here called simply 'Dosino'; Metrohm, Herisau, Switzerland). A Dosino contains a programmable piston that fills and empties a glass cylinder with up to 50 mL of sample at a resolution of 10,000 increments (implying 5 µL increment^{-1}). The design of the dosing unit minimizes the dead volume and thus the potential for sample carryover. In the base of the glass cylinder sits a rotating valve disc that guides the liquid sample through one of four ports; thus each Dosino functions as both a switching valve and a syringe pump.

Figure 1 depicts the schematic overview of the automatic sample collection and analysis system, showing how the different Dosinos distribute precipitation and streamwater samples between the isotope analyzer, the IC and ~~and~~ an autosampler (which can be programmed to save individual samples for subsequent analysis in the laboratory). The sampling routine begins with a cleaning step when either the 'P Dosino' (which handles precipitation) or the 'S Dosino' (which handles streamwater) transports 10 mL of sample water for rinsing to ~~the~~ a sample storage beaker. The 'Isotope Dosinos' also eject any remaining sample into the beaker, after which the beaker is emptied. Then, 50 mL of fresh streamwater or precipitation sample is transported (by either the 'S Dosino' or the 'P Dosino' for streamwater or precipitation, respectively) into the rinsed beaker, from which one of the 'Isotope Dosinos' draws 30 mL of water and injects it at a flow rate of 1 mL min^{-1} into the CWS for isotope analysis. The two 'Isotope Dosinos' operate alternatingly to minimize the time when the sample flow into the CWS is interrupted. Meanwhile, either the 'P Dosino' or the 'S Dosino' takes up another 12 mL of water sample and pumps it through a 0.45 µm tangential filter into the 'IC Dosino', which discards the first 2 mL of the filtered sample. From the remaining filtered sample, 8 mL are filled into vials by the autosampler and 2 mL are delivered to the IC for direct ion analysis. During the ion analysis (ca. 28 min), the 'S Dosino', 'P Dosino' and 'IC Dosino', the autosampler, and all tubing are rinsed with nanopure water to minimize carryover effects. The entire sampling routine is programmed with the IC control software MagIC Net (Metrohm, Herisau, Switzerland), which facilitates detailed data logging and documentation of the sample handling.

3. Laboratory experiments

3.1 Optimization of sample injection into the Continuous Water Sampler module (CWS)

In the original design of the CWS, water samples are transported by a small solenoid diaphragm pump between the inlet port and the membrane cartridge at a flow rate of approximately 1 mL min^{-1}. During preliminary tests, however, we observed that raising or lowering the sample container detectably altered the reported isotope ratios. In order to quantify the sensitivity of the instrument to hydraulic head differences (i.e., the height of the

water table in the sample bottle relative to the waste outlet of the CWS), we changed the elevations of the sample container relative to the instrument while continuously analyzing a single water sample (nanopure water). We measured the vapor concentration, $\delta^{18}O$ and $\delta^{2}H$ for the same water sample at five different elevations, ranging from 7 cm above to 98 cm below the waste outlet. The end of the waste outlet tube was always freely draining. Each configuration was measured for one hour and the average values and standard deviations of the uncalibrated 6 s measurements of vapor concentration, $\delta^{18}O$ and $\delta^{2}H$ were calculated from the last 10 min of each 1 h configuration.

The results of this experiment are summarized in Fig. 2, which shows clear linear relationships between the hydraulic head differences and both the vapor concentrations and the isotope measurements. Lowering the sample source relative to the outflow results in systematically heavier isotopic values in the vapor measured by the instrument. Vapor concentrations show a similar trend, i.e. more vapor was generated for lower positions of the sample source. These observations suggest that the hydraulic head difference directly affected the flow rate of the liquid sample through the CWS membrane tube. Because the water is much colder than the surrounding air as it enters the membrane chamber, it is continuously warming as it travels through the membrane tube. At greater head gradients (and thus smaller flow rates), the sample will travel more slowly through the membrane chamber and will warm up more. As ~~a consequence of~~ higher water temperatures, water ~~can be expected to~~should diffuse more rapidly through the membrane and the resulting vapor ~~can be expected to~~will be less fractionated relative to the liquid phase (Kendall and McDonnell, 1998), as observed in Fig. 2.

It is unknown whether the empirical linear relationships shown in Fig. 2 are generally applicable, or are specific to each individual membrane or to the properties of the sample. Nevertheless, for this membrane and this sample, the results indicate that changing the hydraulic head by 50 cm changes the reported isotope values by approximately 0.12 ‰ for $\delta^{18}O$ and 0.52 ‰ for $\delta^{2}H$, respectively. This flow-rate artifact might become particularly important for applications in which isotope standards and samples are drawn from sample containers at different elevations relative to the waste outlet of the CWS (e.g. shipboard sampling). In such cases, a vapor concentration correction relative to a reference height would have to be carried out ~~to account for the changes in flow rate that affects the isotopic composition in the measured water vapor~~. Alternatively, a different injection system could be used to deliver a specified flow rate, independent of the position of the source relative to the CWS. We used the Dosino for this purpose, since it functions as a high-precision syringe pump whose delivery rate is specified by the pulse rate of the stepper motor, independent of the hydraulic head gradient.

Because of the limited volume of each Dosino's glass cylinder (50 mL), a sample could be injected at a flow rate of 1 mL min^{-1} for a maximum of 50 min. For longer injections, or to switch samples, a second Dosino had to take over the sample delivery. The handoff between the Dosinos interrupted the sample flow to the CWS for around 2 s. This interruption was reflected in a sharp but brief increase in vapor concentrations and isotope values, which returned back to stable values approximately 10 min after the injection started (see Fig. 3 for an example). For our application, i.e. synchronous IC measurements, we programmed a 30 min injection period for the isotope analysis. To obtain the final isotope values of a liquid sample we averaged the individual 6 s

measurements reported by the WS-CRDS during the last 10 min of each 30 min injection period, using the first 20 min to minimize any memory effects from the previous sample or from Dosino changeover. The advantage of the Dosino-based sample ~~injection~~ handling system is the very steady, pressure-independent sample injection.

3.2 Performance of the isotope analyzer with Continuous Water Sampler (CWS)

We quantified precision, drift coefficients and carryover effects of the isotope analyzer with CWS and Dosino-based sample injection, using a continuous 48-hour laboratory experiment that alternated between three water samples (i.e., to mimic streamwater, precipitation and a reference standard). The sample handling system was as shown in Fig. 1, except that the precipitation collector was replaced with a 10 L bottle of nanopure water and the streamwater sampler was replaced by a 10 L bottle of tap water. The sampling system alternated between these two sources, and for each eighth injection it introduced an isotopically heavier secondary standard (Fiji bottled water) (Fig. 3). The isotopic differences between Fiji bottled water and tap water were about (±~~1~~ standard error, *SE*) 4.54 ± 0.02 ‰ and 32.67 ± 0.08 ‰ for $\delta^{18}O$ and $\delta^{2}H$, respectively. The isotopic differences between tap water and nanopure water were much smaller (0.05 ± 0.01 ‰ for $\delta^{18}O$ and 0.12 ± 0.03 ‰ for $\delta^{2}H$) because the nanopure water was generated from the same tap water by reverse osmosis.

The precisions of the isotope values, as quantified by the standard deviations of the individual 6s measurements during the last 10 min of each injection period, were better than 0.08 ‰ for $\delta^{18}O$ and 0.18 ‰ for $\delta^{2}H$. These standard deviations imply that the standard errors of the 10 min averages should be better than 0.008 ‰ and 0.018 ‰ for $\delta^{18}O$ and $\delta^{2}H$, respectively. These standard errors overestimate the repeatability of successive measurements, however. As a measure of sample-to-sample repeatability, the standard deviations of the 10 min averages for the entire 48-hour experiment were 0.03 ‰ ($\delta^{18}O$) and 0.17 ‰ ($\delta^{2}H$), or better, for each of the three water samples (excluding two outliers associated with an interruption in the sampling routine), much larger than the calculated standard errors. Thus, the major uncertainties in the 10 min averages do not arise from the counting statistics of the instrument itself, but rather, we suspect, from sample-to-sample variability in the performance of the vaporizer. We use these larger estimates of uncertainty (0.03 ‰ for $\delta^{18}O$ and 0.17 ‰ for $\delta^{2}H$) in the error propagation calculations presented in Section 5.1.

Instrument drift was analyzed by linear regression of the 10 min averages from the ends of each 30 min injection period. Instrument drift for $\delta^{18}O$ was statistically indistinguishable from zero for two of the three waters, averaging (±~~1~~*SE*) -0.009±0.008, -0.009±0.006, and -0.015±0.007 ‰ day^{-1} for Fiji, nanopure, and tap water, respectively. Instrument drift for $\delta^{2}H$ was slow but statistically significant for two of the three waters, averaging 0.133±0.040, 0.084±0.016, and -0.021±0.021 ‰ day^{-1} for Fiji, nanopure, and tap water, respectively. Thus, the accumulated drift over one day was typically smaller than the measurement precision for individual 10 min averages for either isotope. As explained in Section 4.2 below, substantially faster drift occurred during the field experiment ~~due to biofilm growth on the membrane~~ that ~~, but~~ could, however, ~~be~~ easily be measured and corrected using regularly injected reference standards. This faster drift can be explained with biofilm growth on the membrane, which could be observed on the inside of the membrane tube during preliminary tests with streamwater samples at the field site.

Between-sample memory mainly arises from small remnants of previously injected samples that remain in the sample handling system (e.g., tubes, membrane, valves, pumps) or the analyzer itself, and are carried over to the following analysis. We quantified the between-sample memory effect of the isotope analyzer using two isotopically contrasting samples, Fiji water and nanopure water. The true isotopic difference was obtained from the 7th (=last) injection of nanopure water, which was measured around 3 h after the reference standard (Fiji), and was thus assumed to be free of any memory effects. We calculated the memory coefficient (X) as a measure of carryover effects using Gupta et al. (2009):

$$X = \frac{C_i - C_{i-1}}{C_{true} - C_{i-1}} \quad (1)$$

where C denotes the isotope ratio (or the solute concentration), the indices (i) and (i-1) denote the current and the previous injection, and (*true*) denotes the true value taken from the last value of multiple injections. Based on the 10 min averages from the end of each 30 min injection period, t~~T~~he average carryover from the Fiji bottled water to the next ~~30min~~ sample was 100%·(1-X)≈0.9 % for $\delta^{18}O$ and 1.2 % for $\delta^{2}H$, respectively (Table 1). The carryover during the first and second 10 min of each 30 min injection period was, however, much larger (up to 53 % and 6 %, respectively) implying that our 30 min sampling cycle is indeed necessary to prevent unacceptably large carryover effects.

3.3 Performance of the ion chromatograph (IC)

With the IC, a 48~~h~~-hour laboratory experiment was carried out as well. However, the sampling sequence differed slightly from that of the isotope analyzer described previously: each measurement of tap water or Fiji water was followed by two to six samples of nanopure water, which mimics precipitation samples with generally very low solute concentrations. Due to the low solute concentrations in the nanopure water, carryover effects can be quantified efficiently.

Average concentrations~~,~~ of the major anions and cations during the ~~48h~~48-hour experiment are reported in Table 1, along with their absolute and relative standard deviations. For tap water and Fiji water, relative standard deviations were <5% for all constituents with concentrations above the limit of quantification (LOQ) and ~1% or less for most major ions, indicating that the IC measurements were stable over the ~~48h~~48-hour period and that they were sufficiently precise to detect even subtle biogeochemical signals in streamwater. D~~. Consequently, d~~rift effects in the instrument were not statistically significant ($p>0.05$) for most constituents in Fiji water and tap water. For Cl^-, NO_3^- and SO_4^{2-} in the Fiji water, the linear drift was statistically significant but also very slow: accumulated drift over 24h was never much larger than the LOQ (Table 1). Average % carryover (100%·(1-X), Eq. (1)) in the nanopure water sample, following immediately after a tap water or Fiji water sample, was ≤ 3.8 %.

4. Application in the field

4.1 Setup

For the field experiment, the system was installed in a hut (area 1.7x1.7m) next to a small perennial stream flowing behind the Swiss Federal Institute for Forest, Snow and Landscape Research (WSL) near Zurich, Switzerland. The creek drains an area mainly covered with open grassland, grain fields, and suburban

residential neighbourhoods (Fig. 4). The dominant soil type is colluvial, partly gleyic brown soil (GIS-ZH, 2016).

Stream stage, temperature and electrical conductivity of streamwater were recorded in the stream every 10 min using a data-logging sonde (model DL/N 70; STS SensorTechnik Sirnach, Switzerland). The volumetric discharge was not gauged, but we assume that the times of the highest stream stage coincided with peak flow, and thus use both terms synonymously. Once a day at 7:30 am, daily p~~P~~recipitation ~~(rainfall and snow)~~ was ~~measured~~ measured with a~~n~~ ~~un~~heated collector and snow depth was recorded~~daily at 7:30am~~. For a higher temporal resolution~~,~~ we used the hourly CombiPrecip dataset (MeteoSwiss), a grid-data product that combines radar estimates and rain-gauge measurements to compute precipitation rates at 1 km^2 spatial resolution. A ~~the site were estimated as the average of 10min measurements at three nearby weather stations (Stetten, Zurich Fluntern, and Zurich Affoltern) in the MeteoSwiss observation network. g~~Good agreement (R^2 ~~>~~ = 0.~~82~~86) ~~was observed~~ between measured daily precipitation at our field site and the daily sums of hourly ~~the averages of the three MeteoSwiss stations~~CombiPrecip data ~~, thus~~ indicat~~e~~~~ing~~ that the ~~MeteoSwiss~~ CombiPrecip ~~data~~ dataset ~~are~~ is a reasona~~l~~ble proxy for precipitation ~~rates~~ variability at the field site. To distinguish rain and snowfall events, air temperature was recorded near the instrument hut every 10 min (Haeni, 2016; Schaub et al., 2011). The uninsulated hut was not temperature controlled; however, the instruments produced heat so that inside air temperatures were on average 12°C higher than outside. Outside air temperature variations were reflected inside the hut, where air temperatures ranged from 7 to 23°C.

A submersible pump (Eheim GmbH, Deizisau, Germany) continuously pumped streamwater at a rate of 6 L min^{-1} into a through-flow bucket inside the hut. The volume of the bucket was 10 L; thus every several minutes the contents of the bucket were effectively exchanged. Every 30 min, water was drawn from the bucket by the 'S Dosino' through a 1µm cellulose filter to supply the isotope analyzer, IC and autosampler (Fig. 1). Precipitation was collected with a heated 45 cm diameter funnel installed 2.5 m above ground. Precipitation flowed into a Teflon®-coated collector with a level detector ~~that triggered at a threshold volume of 72 mL (equaling roughly 0.5 mm of precipitation)~~. The status of the level detector was queried before the end of each measurement routine and a precipitation sample was ~~drawn~~ taken only if the threshold volume of 72 mL (equaling roughly 0.5 mm of precipitation) was exceeded. For initial filtration of the precipitation sample, a ceramic frit filter was attached on the suction tube of the 'P Dosino' that drew the sample from the precipitation collector. After precipitation was sampled, a peristaltic pump emptied the precipitation collector to avoid mixing fresh and old precipitation samples. The sampling routine was programmed to always alternate between streamwater and precipitation samples in order to obtain enough streamwater samples during storm periods. To reduce biofilm growth on the membrane in the CWS, copper wool was placed in the beaker from which the 'Isotope Dosinos' drew the samples. Sampling was interrupted approximately once a week for basic maintenance (i.e., replacing the filter membranes, cleaning Dosinos, refilling reference standards and eluent stock solutions).

To correct for instrument drift, internal r~~R~~eference standards were analyzed every 3h ~~to correct for instrument drift~~. ~~Correction for drift was carried out~~ F~~f~~or the five samples between two bracketing measurements of the same reference standard following equation was applied:

$$C_{corr} = C_{raw} + (C_{true} - \frac{C_{std,i}+C_{std,j}}{2}) \quad (2)$$

with C denoting the solute concentration or the isotope ratio, respectively. The indices represent the corrected value (*corr*), the current raw measurement (*raw*), the true value of the reference standard (*true*), and the previous and successive measurements of the same reference standard (*std*) measured at time i and 3h later at time j. For the isotope analyzer, Fiji bottled water was used as ~~drift control~~internal reference standard, which was injected directly from a container by one of the 'Isotope Dosinos' (Fig. 1). The measurements of the IC were drift-corrected with another reference standard (Evian bottled water) ~~in the autosampler~~that was transferred directly to the IC by the 'IC Dosino'. Evian bottled water was used, as its mineral composition resembles that of streamwater more closely than Fiji bottled water does.

4.2 Temporal high-resolution measurements of stable isotopes and major ions in precipitation and streamwater

The measurement system was deployed at the field site from 13 February 2016 to 11 March 2016 and more than 1000 streamwater and precipitation samples were analyzed for stable water isotopes and major ions. ~~. Although the field-based measurement period covered only around 1 month, this real-time analysis system~~ capturinged a wide range of hydrological and hydrochemical conditions. Table 2 provides an overview of the eight storm events during that period. ~~A comparison of the aggregated precipitation data with the on-site daily measurements from the un-heated rainfall collector indicated that~~ Air temperature measurements at the site and daily observations of the snow height showed that pprecipitation during Events #1-#7 was mostly rainfall. ~~S~~Snowfall occurred occasionally after 1 March, while during Event #8 most precipitation fell as snow.

We calculated the response time of streamflow as the time difference between the first detection of precipitation and the first significant increase in streamwater level relative to the initial conditions. ~~Typical R~~response times were between 0 h and 2.5 h (Table 2), suggesting ~~an influence~~fast runoff from the residential area in the eastern part of the catchment. The most ~~A more~~ delayed streamflow response (~~4h~~2.5h) was observed after the snowfall E~~e~~vent ~~(~~#8~~)~~, reflecting delayed snowmelt. As illustrated by Fig. 5, a 30 min sampling interval was sufficient to resolve the temporal patterns of stable isotopes and solutes in streamflow during the rising limb of the hydrograph, even during low-intensity precipitation periods such as Event #5.

Compared to the laboratory experiment with the isotope analyzer, during the field experiment we observed carryover effects in the isotope measurements of up to 100%·(1-X)=3%, which can be explained by the copper wool in the beaker from which the "Isotope Dosinos" drew the water samples. Despite the rinsing routine of the beaker, the wool retained small volumes of sample from previous injections that affected the isotopic composition in the fresh sample. Consequently, the wool was removed and the prior isotope measurements were adjusted with X=97% and Eq. (1). Further, instrument drift was substantially faster during the beginning of the field experiment due to biofilm growth in the membrane tube. For instance, during the first week, instrument drift for raw $\delta^{18}O$ and $\delta^{2}H$ measurements in Fiji bottled water was statistically significant, averaging

(±~~1~~*SE*) -0.185±0.006 and -0.288±0.015 ‰ day^{-1}, respectively. The variations of air temperature outside and inside the hut were not reflected in the isotope measurements because the CWS regulates inlet air and water temperatures using Peltier thermoelectric controllers.

Figure 6a ~~depicts~~ illustrates that~~the local meteoric water line obtained from the isotopic measurements in precipitation. T~~ the isotopic composition of precipitation varied over a range of ~~14.9~~ 15.72 ‰ in $\delta^{18}O$ and 11509~~09~~.634 ~~4~~ ‰ in $\delta^{2}H$. By capturing many precipitation events over weeks to months, our isotope analysis system provides a more detailed insight into the variability of precipitation isotopes compared to previous studies that only monitored individual storms at high frequency (e.g., Moerman et al., 2013; Pangle et al., 2013; Tweed et al., 2016). At our site, a~~A~~ correlation between air temperature and the isotopic composition of precipitation is evident ~~during~~ for most storm events. Figure 5 shows that, for instance, precipitation samples became isotopically heavier during Events #2 and #8 when air temperature increased, while the precipitation samples became isotopically lighter ~~opposite behavior was observed~~ during Events #1, #3 and #5, when air temperature decreased. During Events #4, #6 and #7, however, the correlation with temperature was not as distinct as during the other five events. ~~Moerman et al., 2013Pangle et al., 2013Tweed et al., 2016~~

The isotopic composition of streamwater varied by less than half as much as that of precipitation, i.e. by ~~5~~6.24~~.9~~ ‰ for $\delta^{18}O$ and by 45.11~~43.6~~ ‰ for $\delta^{2}H$, respectively (Fig. 6b). For all eight events, the isotopic signature of pre-event streamwater was relatively constant, averaging -110.0489±0.21 ‰ for $\delta^{18}O$ and -764.9788±1.460 ~~0~~ ‰ for $\delta^{2}H$, respectively (±~~1~~ standard deviation, n=8). During the events, $\delta^{18}O$ and $\delta^{2}H$ in streamwater changed by up to 4.8054 ~~4~~ ‰ and 364.3843 ~~3~~ ‰, respectively (Event #7).

For the IC, memory effects were negligible during the field experiment (because the sample did not make contact with the copper wool), so the measurements were corrected only for drift effects. Solute concentrations in precipitation and streamwater varied widely, as shown for instance in Fig. 5~~ for Cl^- and NO_3^-~~. For Li^+, NH_4^+, K^+, F^- and PO_4^{3-} in streamwater, as well as concentrations of Mg^{2+} in precipitation, measured concentrations were generally below the LOQ. Ca^{2+}, NO_3^- ~~(as well as Ca^{2+}~~ and SO_4^{2-}~~, not shown)~~ in streamwater exhibited clear dilution patterns during all precipitation events (Fig. 5e-~~d~~g). Concentrations of Ca^{2+}, NO_3^-~~, Ca^{2+}~~ and SO_4^{2-} in precipitation during the eight events were on average (±~~1~~ standard deviation) 12.1±2.9 mg L^{-1}, 1.5±1.1 mg L^{-1}~~, 12.1±2.9 mg L^{-1}~~ and 0.5±0.8 mg L^{-1}, respectively. Solute concentrations in pre-event streamwater were on the order of (±~~1~~ standard deviation) 160.8±9.7 mg L^{-1} for Ca^{2+}, 11.7±1.8 mg L^{-1} for NO_3^-~~, 160.8±9.7 mg L^{-1} for Ca^{2+}~~ and 21.5±3.3 mg L^{-1} for SO_4^{2-}, whereas concentrations during ~~all~~ storm events dropped to values as low as 64.6 mg L^{-1} (Ca^{2+}), 3.73 mg L^{-1} (NO_3^-)~~, 64.6 mg L^{-1} (Ca^{2+})~~ and 5.12 mg L^{-1} (SO_4^{2-}). In contrast, EC and the concentrations of Cl^- (and Na^+, not shown) in streamwater showed dilution patterns until Event #3, and then showed distinct enrichment patterns ~~occurred~~ thereafter (Fig. 5d~~e~~), likely associated with road salt wash-off. Due to possible road-salt effects on Na^+ and Cl^-, we will focus on Ca^{2+}, NO_3^- and SO_4^{2-} in the analysis below.

5. Comparison of event-water fractions estimated from isotopices and chemical tracers

5.1 Hydrograph separation methodology and uncertainty analysis

To illustrate a potential application of high-frequency isotope and chemical measurements, here we quantify the event-water fractions during the ~~eight~~ major events captured during the 1-month observation period. We used two-component end-member mixing analysis ~~to quantify the fractions of event water in streamflow during the precipitation events. We~~by applying~~ied~~ the conventional mass balance equation (Pinder and Jones, 1969):

$$F_E = \frac{Q_E}{Q_S} = \frac{C_S - C_P}{C_E - C_P} \quad (3)$$

The fraction of event water relative to total streamflow ($F_E = Q_E/Q_S$) was calculated from the isotope values or solute concentrations in total streamflow (C_S), event precipitation (C_E) and pre-event streamflow (C_P). Here, C_P was obtained for each event from the average of the five streamwater samples immediately before the onset of precipitation. The value of C_E was the incremental, volume-weighted mean (McDonnell et al., 1990) of all precipitation samples that were collected before the respective streamflow sample:

$$C_{E,j} = \frac{\sum_{i=k}^{j} P_i C_i}{\sum_{i=k}^{j} P_i} \quad (4)$$

with P_i being the precipitation depth associated with the isotope value (or solute concentration) C_i collected at time i since the starting time k of the precipitation event.

Uncertainty in the hydrograph separation was quantified with Gaussian error propagation (Genereux, 1998), using calculated standard errors (SE) arising from analytical uncertainties and the temporal variability of the isotope values (or solute concentrations). Because C_E is a volume-weighted mean, the standard error SE_{CE} is calculated with

$$SE_{C_{E,j}} = \left[\frac{\sum_{i=k}^{j} P_i (C_i - C_{E,j})^2}{(j-k) \sum_{i=k}^{j} P_i} \right]^{\frac{1}{2}} \quad (5)$$

where $C_{E,j}$ denotes the volume-weighted mean, C_i denotes the i^{th} concentration that comprises that mean, and (j) is the number of samples included in the volume-weighted mean. The standard error of C_S, SE_{CS}, arises from the measurement uncertainties given in Table 1. For SE_{CP}, the same measurement uncertainties are applied, as well as the temporal variability of the five measurements comprising C_P. The standard error of the event-water fraction (SE_{FE}) can then be obtained by Gaussian error propagation:

$$SE_{F_E} = \left\{ \left[\frac{-1}{C_P - C_E} SE_{C_S} \right]^2 + \left[\frac{C_S - C_E}{(C_P - C_E)^2} SE_{C_P} \right]^2 + \left[\frac{C_P - C_S}{(C_P - C_E)^2} SE_{C_E} \right]^2 \right\}^{1/2} \quad (6)$$

~~The varied weather conditions during the 28-day field experiment led to complex hydrologic responses, resulting in a data set that illustrates the potential of these high-frequency measurements for hydro-chemical analyses. Mixing analysis for two end-members, event water and pre-event water, was carried out for eight storm events between 20 February and 8 March 2016, based on isotopic and chemical tracers. Event #8, where precipitation fell partly as snow, was included in the analysis as river discharge and streamwater EC responded within 4h after the onset of precipitation (Table 2). Hence, the temporal change in the snowmelt isotopic signal due to fractionation was assumed to be negligible.~~ Isotope hydrograph separation (IHS) was performed using both $\delta^{18}O$ and $\delta^{2}H$, whereas chemical hydrograph separation (CHS) was carried out with the three constituents Ca^{2+}, NO_3^- and SO_4^{2-} (Cl^- and Na^+, were not used for CHS due to the influence of road salt at the site) and ~~. We~~

~~also performed hydrograph separation based on~~ streamwater EC. EC was used here~~,~~ since several studies ~~have used~~apply EC in lieu of chemical concentrations for hydrograph separation, owing to the ease of obtaining continuous EC measurements (e.g., Dzikowski and Jobard, 2012; Matsubayashi et al., 1993; Muñoz-Villers and McDonnell, 2012; Pellerin et al., 2008). As we did not measure EC in precipitation directly, we had to estimate it empirically. For this, we used a standard conversion equation, i.e., the pseudo-linear approach following Sposito (2008), to calculate EC in precipitation from the ionic strength of the major cations and anions in the precipitation samples. We assume that the ion concentrations measured by the IC account for the great majority of the ionic strength. In order to estimate the uncertainty of this method, we also calculated the EC values in streamwater and compared them with the actual measurements of the EC probe in the stream. The (absolute value) difference between the calculated and measured streamwater-EC values averaged 20 µS cm^{-1}.

For the uncertainty analysis of the calculated event-water fractions, analytical uncertainties ~~of~~ in the isotope measurements were assumed to be 0.03 ‰ and 0.17 ‰ for $\delta^{18}O$ and $\delta^{2}H$, respectively (Section 3.2, Table 1). Relative uncertainties ~~of~~ in the IC measurements were $0.006 \cdot C + 0.087$ mg L^{-1} for Ca^{2+}, $0.028 \cdot C + 0.002$ mg L^{-1} for NO_3^- and $0.037 \cdot C + 0.006$ mg L^{-1} for SO_4^{2-}, respectively (~~(~~where C is concentration in mg L^{-1}; Table 1). For the EC values, a measurement uncertainty of 2 % was assumed for the EC probe based on the specifications given by the EC probe's manufacturer. The assumed uncertainty in the EC values in precipitation was 20 µS cm^{-1}, as calculated above.

5.2 Event-water fractions for eight storm events

Mixing analysis for two end-members, event water and pre-event water, was carried out for eight storm events between 20 February and 8 March 2016, based on isotopic and chemical tracers. Event #8, where precipitation fell partly as snow, was included in the analysis ~~as~~because river discharge and streamwater EC responded within 4h after the onset of precipitation (Table 2). Hence, the temporal change in the snowmelt isotopic signal due to fractionation was assumed to be negligible. Two ~~illustrative precipitation~~storm events are analyzed in more detail, followed by a general discussion of the hydrograph separation results based on all eight events.

Two storm events

Figures 7 and 8 show the ~~, together with their~~ hydrologic, isotopic and chemical responses in streamwater and precipitation during~~, are shown in Figs. 7 and 8 (~~Events #1 and #2, respectively~~)~~. During Event #1, total rainfall was ~~6.7~~ 6.8 mm within 6~~10~~h ~~40min~~, while 1 1~~0~~.5~~3~~ mm rain fell within 13~~9~~h ~~40min~~ during Event #2. Antecedent moisture conditions, ~~estimated~~ as inferred from~~by~~ the total rainfall within 48 h and 24 h before the event, as well as initial streamwater level, were relatively wet for Event #1 and relatively dry for Event #2 (Table 2).

For Event #1, $\delta^{18}O$ and $\delta^{2}H$ in streamwater followed the observed patterns in precipitation, i.e. streamwater became isotopically lighter over time. Isotope hydrograph separations (IHS) for this event yielded maximum event-water fractions ($F_{E,max}$) of 80~~78~~±1 1~~0~~ % and 59~~60~~±14 % for $\delta^{18}O$ and $\delta^{2}H$, respectively, similar to the results obtained from the chemical tracers Ca^{2+}, NO_3^- and SO_4^{2-} (57±1 %, 65±2 % and 65±3 %) and EC (56±3 %, Fig. 7d and e). The larger uncertainties of the IHS compared to CHS can be explained with the large temporal variability of the isotope values in precipitation, which substantially exceeds analytical uncertainty.

During Event #1~~T~~, the fraction of event water increased rapidly after the start of rainfall and declined continuously as stream stage receded. A difference in ~~response~~ timing of $F_{E,max}$ ~~is~~ was evident for ~~the chemical and isotope~~both tracer types~~s~~ ~~in~~ (Fig. 7d~~- and 7~~e): $F_{E,max}$ based on t~~T~~he chemical tracers ~~exhibited the strongest dilution effect~~occurred ~~during~~ 1 h after peak flow, whereas $F_{E,max}$ based on the isotope tracers was ~~showed the largest response to the event~~ roughly 3~~2~~h ~~later~~delayed, possibly because the isotopic signature in precipitation became lighter as the event progressed. Consequently, if C_S ~~–~~values at the time of peak flow ~~Q_{max}~~ were used to perform hydrograph separation (Eq. (3)), isotope-based F_E-values would be substantially smaller (i.e., 13~~43~~±~~46~~ % and 15~~42~~±~~39~~ % for $\delta^{18}O$ and $\delta^{2}H$, respectively) than the $F_{E,max}$-values reported above.

During Event #2, the solutes in streamwater showed a clear dilution signal (Fig. 8c), similar to Event #1. The isotopic composition in streamwater, by contrast, showed only a very weak and inconsistent response to precipitation. For instance, $\delta^{2}H$ in precipitation increased continuously through the event, whereas $\delta^{2}H$ in streamwater first decreased and then, ~~ca. 4 h~~several hours after the onset of precipitation, began to increase again. Consequently, IHS and CHS yielded substantially different interpretations for Event #2. Maximum event-water fractions based on CHS ranged from 6~~7~~8±1 % (Ca^{2+}) to 8~~2~~3±~~3~~5 % ($SN~~O~~O_4^{2-}$), similar to Event #1. In contrast, $F_{E,max}$-values based on IHS ranged from 8~~7~~±1 % to 15~~6~~±3 %, indicating that pre-event water was the dominant source of streamwater during peak flow.

How can such a large discrepancy between the event-water fractions calculated from different environmental tracers be explained? From Fig. 5 it can be seen that precipitation was isotopically lighter than streamwater during the six days leading up to Event #2. Thus, the initial decrease in the $\delta^{18}O$ and $\delta^{2}H$ values in streamwater during Event #2 suggests the release of isotopically lighter soilwater and groundwater that were recharged during previous events. An activation of this pre-event water storage might have been triggered by enhanced infiltration after relatively dry antecedent moisture conditions (AMC), compared to the previous event, whereas wet AMC would be more consistent with surface runoff generation. This hypothesis is further supported by the isotopic responses in streamwater during Event #5, another isotopically heavy event with dry AMC, following earlier inputs of isotopically lighter precipitation. In Event #5, small event-water fractions (12±1 % and 2~~0~~±1 % for $\delta^{18}O$ and $\delta^{2}H$, respectively; Fig. S1) were again obtained, indicating that pre-event water dominated streamflow, similarly to Event #2. And in Event #5, just as in Event #2, the chemical tracers showed strong dilution, leading to an overestimate of the maximum event-water fraction (>40±2 %). In both Event #2 and Event #5, the chemical and isotopic data ~~point~~ indicate ~~to~~ a large contribution from recent ~~antecedent moisture~~soilwater or groundwater that had not yet become highly mineralized, rather than from either event precipitation or from older groundwater that presumably accounted for most of the pre-event baseflow.

General discussion of hydrograph-separation results

Figure 9 summarizes the estimated event-water fractions for all eight events, based on IHS and CHS, for two points in time during each event: the time with the largest isotopic or chemical response (i.e., $F_{E,max}$) and the time of peak flow ~~(Q_{max})~~. Maximum event-water fractions varied greatly across the eight events (for example, from 1~~5~~6±3% to 73~~68~~±1~~7~~4% based on $\delta^{2}H$, Fig. 9, Table S1 and S2). Also, within individual events, hydrograph separations based on different isotopic and chemical tracers differed, often by much more than their

uncertainties. Inconsistencies between the estimated event-water fractions can be explained with the fact that different tracers are shaped by different hydrochemical processes and flow pathways, and thus may describe different end-members (e.g., Richey et al., 1998; Wels et al., 1991). While stable water isotopes are considered to be ideal conservative tracers, chemical tracers are altered by biogeochemical processes on their way through ~~a~~ hydrological systems. These biogeochemical processes also vary over time, as they depend on antecedent conditions and precipitation characteristics. ~~Continuous~~ Hhigh-frequency analysis of environmental tracers can document this temporal variability, which, in turn, helps to constrain conceptual catchment models. As illustrated by Events #2 and #5, comparing chemical and isotopic tracers can be useful in identifying the temporally variable contributions of different water storages in the subsurface.

For Event #7, IHS based on $\delta^{18}O$ resulted in event-water fractions >100%, which can be explained by the fact that the first precipitation sample of this event was isotopically very similar to the pre-event water signature (C_E=-11.69‰, C_P=-11.09‰). The incremental, volume-weighted mean of the event-water end member was thus isotopically heavier than the streamwater end member, resulting in a smaller difference from the pre-event water end member signature (Eq. 3). Precipitation samples after this first, less-$\delta^{18}O$-depleted sample had an average $\delta^{18}O$ value of -16.86±0.73‰ (±standard deviation, n=6). For $\delta^{2}H$, such a strong effect did not occur and we could obtain reasonable isotope-based hydrograph separation results similar to the chemical hydrograph separation.

Figure 9 illustrates further that for three events (#2, #5 and #8), estimated event-water fractions for the two isotopes, $\delta^{18}O$ and $\delta^{2}H$, differed significantly (i.e., by more than twice their pooled uncertainties). These differences did not follow any particular pattern, for instance, $F_E(\delta^{18}O) > F_E(\delta^{2}H)$ for Event #8, while $F_E(\delta^{18}O) < F_E(\delta^{2}H)$ for Events #2 and #5. ~~A possible explanation for~~ Ssuch discrepancies ~~is~~ might be caused by temporally variable $\delta^{18}O$-$\delta^{2}H$ relations (d-excess) of contributing water sources (groundwater, soil water, overland flow), resulting in different event-water fractions based on both isotopes. An alternative explanation is that ~~the isotopic signature of precipitation sampled at one location might not be representative of the spatially distributed precipitation that generated the sampled streamflow (e.g., Fischer et al., 2015; Lyon et al., 2009). Alternatively,~~ the pre-event streamflow signature (C_P) may not reflect the isotopic signature of the entire pre-event water storage, but only of the components that feed baseflow (e.g., Klaus and McDonnell, 2013). Another way of viewing this problem is that the precipitation event may have mobilized a third pre-event water storage with unknown isotopic composition (e.g., Tetzlaff et al., 2014). This conjecture is strongly supported by the initial shift toward isotopically lighter streamflow early in Event #2, even though the event precipitation was isotopically heavier than the pre-event baseflow. Event #5 also show~~s~~ed divergent event-water fractions between the two isotopes, and like Event #2, it also had strongly contrasting pre-event precipitation inputs. Thus, the history of both events suggests that pre-event storage in this catchment was isotopically heterogeneous. This observation is unsurprising, given the pervasive heterogeneity of typical catchments, but a more detailed explanation is not possible with our spatially limited data set. Spatially distributed measurements, such as from groundwater and soil water storages, would help in constraining the individual end-members that contribute to streamflow (e.g., Hangen et al., 2001). Additional high-frequency time series of the groundwater table and soil moisture profiles would allow for documenting the effects of antecedent wetness conditions on the response times and on the activation of different storages at the site. Finally, a spatially distributed precipitation

sampling network might help to fully quantify the uncertainty inherent in the event-water signature (e.g., Fischer et al., 2017 ~~Fischer et al., 2016;Fischer et al., 2017~~; Lyon et al., 2009).

~~5.3 Variable response times of chemical and isotope tracers~~

~~Measuring isotopes and solutes at high temporal resolution over several storm periods allows for a detailed investigation of response times of hydrological and hydrochemical variables and their linkages to the event characteristics. As can be seen for instance in Fig. 7, during Event #1 the timing of the largest hydrological and hydrochemical responses did not always coincide. For only three events (i.e., #2, #4, #6) the timing of peak flow coincided with the $F_{E, max}$ values for both chemical and isotope tracers. During Event #3, the isotope tracers resulted in $F_{E, max}$ values 1.5h±1.0 h before peak flow. For Events #7 and #8, which were affected by snowmelt, both tracer types showed the strongest responses up to 2.0±1.0 h earlier than the actual flow peak. In contrast, during Event #1 the peak responses in the isotope tracers and EC came up to 2.0h±1.0 h after peak flow.~~

~~These examples illustrate that the hydrological conditions of the stream (i.e., the stream stage or flow rate) are not reliable proxies for the timing of the maximum event water contribution. As a consequence, collecting samples only during or after peak flow may result in a significant underestimation of event water fractions. Our data indicate that the time window for sample collection at our site must extend more than 3h before and after peak flow in order to capture the whole range of event water dynamics. In the case of the snowmelt Event #8, the EC data suggest an even longer sampling period in order to capture unusual events such as the inflow of water contaminated by road salt.~~

5.~~4~~ 3 The role of the sampling frequency for capturing hydrological and hydrochemical catchment processes

A sampling frequency can be considered optimal when the gain of information from additional measurements is marginal (Kirchner et al., 2004; Neal et al., 2012). With our high-resolution data set we can thus investigate the potential of different sampling frequencies for capturing hydrological and hydrochemical catchment processes, by subsampling the 30 min time series at smaller sampling frequencies, i.e. at 3-hourly, 6-hourly, 12-hourly and daily intervals. ~~For concentrations and isotope values in streamwater, data were simply sub-sampled from the 30min resolution time series to mimic grab sampling.~~ To mimic the effects of integrated bulk precipitation samples, we calculated the volume-weighted averages of concentrations and isotope values in precipitation ~~were calculated from the volume-weighted averages of the 30min data~~ over the ~~respective~~ corresponding time intervals.

Figure 10 shows that 3 h sampling ~~intervals~~ frequencies would still be sufficient to capture the isotopic variations in streamwater, including during low-intensity precipitation events. However, the short-term variability within single storm periods, as well as the rapid changes in precipitation isotope values, cannot be resolved at this lower sampling frequency. Thus, even sampling intervals of 3 h can result in a significant loss of information relative to 30 min sampling, and at sampling intervals of 12 h or longer, diurnal fluctuations and some isotopic and chemical responses to low-intensity precipitation events would also be lost. Likewise, the 6 h

or 12 h bulk precipitation samples shown in Fig. 10 fail to reflect the large isotopic variability revealed by the 30 min samples.

To further illustrate the effect of lower sampling frequencies, we performed hydrograph separation with the subsampled data sets, for which illustrative results of the maximum event-water fractions are shown for ~~the isotope tracer~~ δ^2H and EC in Fig. 11. With a sampling ~~interval~~ frequency of 3 h, maximum event-water fractions similar to those for the 30 min sampling can still be obtained, except for Events #3 (EC) and #4 (EC) where $F_{E,max}$ is underestimated~~, except for Event #3, when the 3h sampling interval captured a streamwater sample that was isotopically very similar to the pre-event water~~. ~~For Events #2, #3, #5 and #7,~~ L~~l~~onger sampling intervals (6 h, 12 h) result in ~~underestimate event-water fractions. With 12h sampling intervals, IHS with δ^2H yields~~ much smaller event-water fractions for ~~all~~ most events~~ except Event #4, and yields unrealistic results for two Events (#1, #5), as the isotopic differences between the two end-members become too small~~.

Because the hydrologic response times in this catchment were only ~~mostly~~ between 0 h and ~~much shorter than~~ 2.5 h, the durations of the maximum hydrochemical variations were similarly short. ~~As can be seen for instance in Fig. 7, during Event #1 the timing of the largest hydrological and hydrochemical responses did not always coincide. For only three events (i.e., #2, #4, #6) the timing of peak flow coincided with the $F_{E, max}$ values for both chemical and isotope tracers. During Event #3, the isotope tracers resulted in $F_{E, max}$ values 1.5h±1.0 h before peak flow. For Events #7 and #8, which were affected by snowmelt, both tracer types showed the strongest responses up to 2.0±1.0 h earlier than the actual flow peak. In contrast, during Event #1 the peak responses in the isotope tracers and EC came up to 2.0h±1.0 h after peak flow.~~ ~~Thus~~Consequently, sampling at longer time intervals increases the risk of missing this critical peak response; if the sample is taken before or after the maximum hydrochemical response, the event-water signal in streamwater (C_S) may be too weak, which will inevitably underestimate event-water fractions, or even lead to unrealistic negative values. Furthermore, the rapid changes observed in precipitation isotopic composition (Fig. 6) suggests that high-frequency measurements are crucial for adequately representing the signature of the event-water end member. Capturing the short-term responses of environmental tracers also helps in better quantifying transit time distributions (e.g., Birkel et al., 2012; Stockinger et al., 2016; Timbe et al., 2015) and in constraining concentration-discharge models (e.g., Stelzer and Likens, 2006; Jones et al., 2012).

Our data also show that peak flow is not always a reliable predictor for the time when F_E becomes largest. As can be seen for instance during Event #1 (Fig. 7), $F_{E, max}$ based on IHS occurred up to 3.0±1.0 h after peak flow. The timing of peak flow and the $F_{E, max}$ values for chemical and isotope tracers coincided for only four events (i.e., #2, #6, #7, #8). During the remaining events, the tracer signal showed the strongest responses up to 2.5±1.0 h after peak flow, indicating that the time window for sample collection at our site must extend more than 3 h before and after peak flow in order to capture the whole range of event water dynamics. In the case of snowmelt Event #8, when the maximum EC response occurred 5 h before peak flow, an even longer sampling period would be required in order to capture unusual events such as the inflow of water contaminated by road salt.

6 Concluding remarks

This paper presents the first field hydrology application of Picarro's Continuous Water Sampler (CWS) module, which was coupled to a L2130-*i* Wavelength Scanned-Cavity ring-down Spectrometer to measure ~~the stable water isotopes~~ $\delta^{18}O$ and $\delta^{2}H$ in streamwater and precipitation at a temporal resolution of 30 min. We combined this real-time isotope analysis system with a dual-channel ion chromatograph for synchronous analysis of major cations and anions. Good instrument performance and high measurement precision could be achieved during continuous 48-hour laboratory experiments and a 28-day deployment in the field at a small, partly urbanized catchment in central Switzerland.

Problematic issues such as sample degradation during storage and transportation, which arise in conventional sampling for catchment tracer studies, become irrelevant with the system presented here. At the same time, potential registration errors arising during the collection and handling of large numbers of water samples are avoided. Conversely, two major limitations of the coupled isotope ~~analyser~~ analyzer / IC system are its high cost~~,~~ and the need for ~~sufficient electrical~~line power ~~(around 1.7 kW)~~, constraining its use in remote locations. However, laboratory analysis of conventionally collected grab samples is also cost-intensive, and autosamplers used in conventional sampling schemes also require a reliable energy supply (though at much lower power levels).

The results of the high-frequency analysis system ~~were~~ are presented here to provide a proof-of-concept and an illustration of its functionality at the field, rather than to fully document the hydrological and biogeochemical processes at this field site. A more detailed interpretation would require additional measurements of soilwater and groundwater isotopes and chemistry, in order to better constrain the end-members in the mixing analysis. Nevertheless, our one-month field experiment demonstrates the marked short-term variability of several natural tracers in a small, highly dynamic watershed. The hydrograph separation exercise clearly showed that long-term, high-frequency isotopic and chemical analyses are essential for capturing the "unusual but informative" events that shed light on catchment storage and flow processes. We further showed that the right timing for capturing peak event-water contributions can easily be missed with conventional grab sampling strategies at time intervals longer than 3 h, resulting in an underestimation of the event-water fraction. In addition, the relative timing of the isotopic and chemical responses was highly variable, demonstrating the challenge of capturing the right moments with episodic snapshot campaigns or long-term monitoring with daily, weekly, or even monthly sampling intervals.

As was shown here and elsewhere (e.g., Kirchner, 2003), short-term responses of streamflow and environmental tracers may follow distinctly different patterns, which helps in constraining streamflow-generation~~ng~~ mechanisms and quantifying short transit times. Thus, high-frequency isotopic and chemical measurements also have great potential for catchment model validation. Potential future applications of the system could include sites with rapid hydrologic responses, such as urban streams (e.g., Jarden et al., 2016; Jefferson et al., 2015; Soulsby et al., 2014), wastewater~~-~~ and drinking water systems (e.g., Houhou et al., 2010; Kracht et al., 2007) or agricultural catchments with artificial drainage networks (e.g., Doppler et al., 2012; Heinz et al., 2014). By eliminating errors associated with the handling, transportation and storage of individual bottles, our analysis

system may also achieve better precision than conventional field sampling followed by laboratory analyses. As a result, our system may be able to detect subtle isotopic and biogeochemical signals (associated with, e.g., evaporation effects or in-stream biological processes) that would be missed by conventional approaches to sampling and analysis. Thus, this system can potentially shed new light on the linkages between hydrological, biological, and geochemical processes.

Acknowledgements

We thank Anton Burkhardt and the facilities staff of the Swiss Federal Institute for Forest, Snow and Landscape Research (WSL) for logistical support, and Matthias Haeni from the Long-term Forest Ecosystem Research Programme (LWF) at WSL for providing air temperature data. We also ~~would like to~~ thank Barbara Herstritt of the isotope laboratory at the University Freiburg (Germany) for the analysis of the isotope reference standards, as well as Kate Dennis and David Kim-Hak of Picarro Inc. (Santa Clara, CA, USA) for technical advice.

665

References

Aubert, A. H., Gascuel-Odoux, C., Gruau, G., Akkal, N., Faucheux, M., Fauvel, Y., Grimaldi, C., Hamon, Y., Jaffrezic, A., Lecoz-Boutnik, M., Molenat, J., Petitjean, P., Ruiz, L., and Merot, P.: Solute transport dynamics in small, shallow groundwater-dominated agricultural catchments: insights from a high-frequency, multisolute 10 yr-long monitoring study, Hydrol. Earth Syst. Sci., 17, 1379-1391, 10.5194/hess-17-1379-2013, 2013.

Aubert, A. H., and Breuer, L.: New seasonal shift in in-stream diurnal nitrate cycles identified by mining high-frequency data, PLoS ONE, 11, 10.1371/journal.pone.0153138, 2016.

Bende-Michl, U., and Hairsine, P. B.: A systematic approach to choosing an automated nutrient analyser for river monitoring, Journal of Environmental Monitoring, 12, 127-134, 2010.

Benettin, P., Kirchner, J. W., Rinaldo, A., and Botter, G.: Modeling chloride transport using travel time distributions at Plynlimon, Wales, Water Resour. Res., 51, 3259-3276, 10.1002/2014WR016600, 2015.

Berman, E. S. F., Gupta, M., Gabrielli, C., Garland, T., and McDonnell, J. J.: High-frequency field-deployable isotope analyzer for hydrological applications, Water Resour. Res., 45, 10.1029/2009wr008265, 2009.

Birkel, C., Soulsby, C., Tetzlaff, D., Dunn, S., and Spezia, L.: High-frequency storm event isotope sampling reveals time-variant transit time distributions and influence of diurnal cycles, Hydrol. Process., 26, 308-316, 10.1002/hyp.8210, 2012.

Buso, D. C., Likens, G. E., and Eaton, J. S.: Chemistry of precipitation, streamwater, and lakewater from the Hubbard Brook Ecosystem Study: a record of sampling protocols and analytical procedures, USDA Forest Service, Northeastern Research Station, USDA Forest Service, Newtown Square, PA., Gen. Tech. Rep. NE-275, 52pp, 2000.

Craig, H.: Isotopic variations in meteoric waters, Science, 133, 1702-1703, 1961.

Darling, W. G., and Bowes, M. J.: A long-term study of stable isotopes as tracers of processes governing water flow and quality in a lowland river basin: the upper Thames, UK, Hydrol. Process., 30, 2178-2195, 10.1002/hyp.10779, 2016.

Doppler, T., Camenzuli, L., Hirzel, G., Krauss, M., Luck, A., and Stamm, C.: Spatial variability of herbicide mobilisation and transport at catchment scale: insights from a field experiment, Hydrol. Earth Syst. Sci., 16, 1947-1967, 10.5194/Hess-16-1947-2012, 2012.

Dzikowski, M., and Jobard, S.: Mixing law versus discharge and electrical conductivity relationships: application to an alpine proglacial stream, Hydrol. Process., 26, 2724-2732, Doi 10.1002/Hyp.8366, 2012.

Fischer, B. M. C., van Meerveld, I., and Seibert, J.: Spatial variability in the isotopic composition of rainfall in a small headwater catchment and its effect on hydrograph separation, Journal of Hydrology, http://dx.doi.org/10.1016/j.jhydrol.2017.01.045, 2017.

Genereux, D.: Quantifying uncertainty in tracer-based hydrograph separations, Water Resour. Res., 34, 915-919, 1998.

GIS-ZH: Geographisches Informationssystem des Kantons Zürich (GIS-ZH), Amt für Raumentwicklung, Abteilung Geoinformation, GIS-Produkte GIS-Browser, Map, available at: http://maps.zh.ch/, last access: 4 October 2016, 2016.

Gupta, P., Noone, D., Galewsky, J., Sweeney, C., and Vaughn, B. H.: Demonstration of high-precision continuous measurements of water vapor isotopologues in laboratory and remote field deployments using wavelength-scanned cavity ring-down spectroscopy (WS-CRDS) technology, Rapid Commun Mass Sp, 23, 2534-2542, 10.1002/rcm.4100, 2009.

Halliday, S. J., Skeffington, R. A., Wade, A. J., Neal, C., Reynolds, B., Norris, D., and Kirchner, J. W.: Upland streamwater nitrate dynamics across decadal to sub-daily timescales: a case study of Plynlimon, Wales, Biogeosciences, 10, 8013-8038, 2013.

Hangen, E., Lindenlaub, M., Leibundgut, C., and von Wilpert, K.: Investigating mechanisms of stormflow generation by natural tracers and hydrometric data: a small catchment study in the Black Forest, Germany, Hydrol. Process., 15, 183-199, 2001.

Harman, C. J.: Time-variable transit time distributions and transport: Theory and application to storage-dependent transport of chloride in a watershed, Water Resour. Res., 51, 1-30, 10.1002/2014WR015707, 2015.

Hayashi, M., Vogt, T., Mächler, L., and Schirmer, M.: Diurnal fluctuations of electrical conductivity in a pre-alpine river: Effects of photosynthesis and groundwater exchange, Journal of Hydrology, 450, 93-104, Doi 10.1016/J.Jhydrol.2012.05.020, 2012.

Heinz, E., Kraft, P., Buchen, C., Frede, H. G., Aquino, E., and Breuer, L.: Set Up of an Automatic Water Quality Sampling System in Irrigation Agriculture, Sensors-Basel, 14, 212-228, 10.3390/S140100212, 2014.

Herbstritt, B., Gralher, B., and Weiler, M.: Continuous in situ measurements of stable isotopes in liquid water, Water Resour. Res., 48, 10.1029/2011wr011369, 2012.

Houhou, J., Lartiges, B. S., France-Lanord, C., Guilmette, C., Poix, S., and Mustin, C.: Isotopic tracing of clear water sources in an urban sewer: A combined water and dissolved sulfate stable isotope approach, Water Research, 44, 256-266, 10.1016/j.watres.2009.09.024, 2010.

Jarden, K. M., Jefferson, A. J., and Grieser, J. M.: Assessing the effects of catchment-scale urban green infrastructure retrofits on hydrograph characteristics, Hydrol. Process., 30, 1536-1550, 10.1002/hyp.10736, 2016.

Jasechko, S., Kirchner, J. W., Welker, J. M., and McDonnell, J. J.: Substantial proportion of global streamflow less than three months old, Nature Geoscience, 9, 126-129, 10.1038/Ngeo2636, 2016.

Jefferson, A. J., Bell, C. D., Clinton, S. M., and McMillan, S. K.: Application of isotope hydrograph separation to understand contributions of stormwater control measures to urban headwater streams, Hydrol. Process., 29, 5290-5306, 10.1002/hyp.10680, 2015.

Jones, A. S., Horsburgh, J. S., Mesner, N. O., Ryel, R. J., and Stevens, D. K.: Influence of Sampling Frequency on Estimation of Annual Total Phosphorus and Total Suspended Solids Loads, J. Am. Water Resour. Assoc., 48, 1258-1275, 10.1111/j.1752-1688.2012.00684.x, 2012.

Kendall, C., and McDonnell, J. J.: Isotope tracers in catchment hydrology, Elsevier, Amsterdam ; New York, xxix, 839 p. pp., 1998.

Kirchner, J. W.: A double paradox in catchment hydrology and geochemistry, Hydrol. Process., 17, 871-874, 10.1002/Hyp.5108, 2003.

Kirchner, J. W., Feng, X. H., Neal, C., and Robson, A. J.: The fine structure of water-quality dynamics: the (high-frequency) wave of the future, Hydrol. Process., 18, 1353-1359, 10.1002/Hyp.5537, 2004.

Kirchner, J. W., and Neal, C.: Universal fractal scaling in stream chemistry and its implications for solute transport and water quality trend detection, P Natl Acad Sci USA, 110, 12213-12218, 10.1073/Pnas.1304328110, 2013.

Klaus, J., and McDonnell, J. J.: Hydrograph separation using stable isotopes: Review and evaluation, Journal of Hydrology, 505, 47-64, 10.1016/j.jhydrol.2013.09.006, 2013.

Kracht, O., Gresch, M., and Gujer, W.: A Stable Isotope Approach for the Quantification of Sewer Infiltration, Environmental Science & Technology, 41, 5839-5845, 10.1021/es062960c, 2007.

Leibundgut, C., and Seibert, J.: Tracer Hydrology, in: The Science of Hydrology, edited by: Uhlenbrook, S., Treatise on Water Science, Elsevier, Amsterdam, 215-236, 2011.

Lyon, S. W., Desilets, S. L. E., and Troch, P. A.: Characterizing the response of a catchment to an extreme rainfall event using hydrometric and isotopic data, Water Resour. Res., 44, 10.1029/2007wr006259, 2008.

Lyon, S. W., Desilets, S. L. E., and Troch, P. A.: A tale of two isotopes: differences in hydrograph separation for a runoff event when using delta D versus delta O-18, Hydrol. Process., 23, 2095-2101, 10.1002.hyp.7326, 2009.

Matsubayashi, U., Velasquez, G. T., and Takagi, F.: Hydrograph separation and flow analysis by specific electrical conductance of water, Journal of Hydrology, 152, 179-199, 10.1016/0022-1694(93)90145-Y, 1993.

McDonnell, J. J., Bonell, M., Stewart, M. K., and Pearce, A. J.: Deuterium Variations in Storm Rainfall - Implications for Stream Hydrograph Separation, Water Resour. Res., 26, 455-458, 10.1029/WR026i003p00455, 1990.

McGlynn, B. L., and McDonnell, J. J.: Quantifying the relative contributions of riparian and hillslope zones to catchment runoff, Water Resour. Res., 39, 10.1029/2003wr002091, 2003.

Moerman, J. W., Cobb, K. M., Adkins, J. F., Sodemann, H., Clark, B., and Tuen, A. A.: Diurnal to interannual rainfall δ18O variations in northern Borneo driven by regional hydrology, Earth and Planetary Science Letters, 369–370, 108-119, http://dx.doi.org/10.1016/j.epsl.2013.03.014, 2013.

Munksgaard, N. C., Wurster, C. M., and Bird, M. I.: Continuous analysis of delta O-18 and delta D values of water by diffusion sampling cavity ring-down spectrometry: a novel sampling device for unattended field monitoring of precipitation, ground and surface waters, Rapid Commun Mass Sp, 25, 3706-3712, 10.1002/rcm.5282, 2011.

Munksgaard, N. C., Wurster, C. M., Bass, A., and Bird, M. I.: Extreme short-term stable isotope variability revealed by continuous rainwater analysis, Hydrol. Process., 26, 3630-3634, 10.1002/hyp.9505, 2012.

Muñoz-Villers, L. E., and McDonnell, J. J.: Runoff generation in a steep, tropical montane cloud forest catchment on permeable volcanic substrate, Water Resour. Res., 48, n/a-n/a, 10.1029/2011WR011316, 2012.

Neal, C., Reynolds, B., Norris, D., Kirchner, J. W., Neal, M., Rowland, P., Wickham, H., Harman, S., Armstrong, L., Sleep, D., Lawlor, A., Woods, C., Williams, B., Fry, M., Newton, G., and Wright, D.: Three decades of water quality measurements from the Upper Severn experimental catchments at Plynlimon, Wales: an openly accessible data resource for research, modelling, environmental management and education, Hydrol. Process., 25, 3818-3830, 10.1002/hyp.8191, 2011.

Neal, C., Reynolds, B., Rowland, P., Norris, D., Kirchner, J. W., Neal, M., Sleep, D., Lawlor, A., Woods, C., Thacker, S., Guyatt, H., Vincent, C., Hockenhull, K., Wickham, H., Harman, S., and Armstrong, L.: High-frequency water quality time series in precipitation and streamflow: From fragmentary signals to scientific challenge, Sci Total Environ, 434, 3-12, http://dx.doi.org/10.1016/j.scitotenv.2011.10.072, 2012.

Pangle, L. A., Klaus, J., Berman, E. S. F., Gupta, M., and McDonnell, J. J.: A new multisource and high-frequency approach to measuring δ2H and δ18O in hydrological field studies, Water Resour. Res., 49, 7797-7803, 10.1002/2013WR013743, 2013.

Pellerin, B. A., Wollheim, W. M., Feng, X., and Vörörsmarty, C. J.: The application of electrical conductivity as a tracer for hydrograph separation in urban catchments, Hydrol. Process., 22, 1810-1818, 10.1002/hyp.6786, 2008.

Pinder, G. F., and Jones, J. F.: Determination of the ground-water component of peak discharge from the chemistry of total runoff, Water Resour. Res., 5, 438-445, 10.1029/WR005i002p00438, 1969.

Richey, D. G., McDonnell, J. J., Erbe, M. W., and Hurd, T. M.: Hydrograph separations based on chemical and isotopic concentrations: A critical appraisal of published studies from New Zealand, North America and Europe, Journal of Hydrology New Zealand, 37, 95-111, 1998.

Riml, J., and Worman, A.: Spatiotemporal decomposition of solute dispersion in watersheds, Water Resour. Res., 51, 2377-2392, 10.1002/2014WR016385, 2015.

Rode, M., Angelstein, S. H. N., Anis, M. R., Borchardt, D., and Weitere, M.: Continuous In-Stream Assimilatory Nitrate Uptake from High Frequency Sensor Measurements, Environmental Science & Technology, 50, 5685-5694, 2016a.

Rode, M., Wade, A. J., Cohen, M. J., Hensley, R. T., Bowes, M. J., Kirchner, J. W., Arhonditsis, G. B., Jordan, P., Kronvang, B., Halliday, S. J., Skeffington, R. A., Rozemeijer, J. C., Aubert, A. H., Rinke, K., and Jomaa, S.: Sensors in the Stream: The High-Frequency Wave of the Present, Environmental Science & Technology, 50, 10297-10307, 10.1021/acs.est.6b02155, 2016b.

Schaub, M., Dobbertin, M., Krauchi, N., and Dobbertin, M. K.: Preface-long-term ecosystem research: understanding the present to shape the future, Environ Monit Assess, 174, 1-2, 2011.

Soulsby, C., Birkel, C., and Tetzlaff, D.: Assessing urbanization impacts on catchment transit times, Geophysical Research Letters, 41, 442-448, 2014.

Sposito, G.: The chemistry of soils, 2nd ed., Oxford University Press, Oxford; New York, xii, 329 p. pp., 2008.

Stelzer, R. S., and Likens, G. E.: Effects of sampling frequency on estimates of dissolved silica export by streams: The role of hydrological variability and concentration-discharge relationships, Water Resour. Res., 42, 10.1029/2005WR004615, 2006.

Stockinger, M. P., Bogena, H. R., Lücke, A., Diekkrüger, B., Cornelissen, T., and Vereecken, H.: Tracer sampling frequency influences estimates of young water fraction and streamwater transit time distribution, Journal of Hydrology, 541, Part B, 952-964, http://dx.doi.org/10.1016/j.jhydrol.2016.08.007, 2016.

Tetzlaff, D., Birkel, C., Dick, J., Geris, J., and Soulsby, C.: Storage dynamics in hydropedological units control hillslope connectivity, runoff generation, and the evolution of catchment transit time distributions, Water Resour. Res., 50, 969-985, 2014.

Timbe, E., Windhorst, D., Celleri, R., Timbe, L., Crespo, P., Frede, H. G., Feyen, J., and Breuer, L.: Sampling frequency trade-offs in the assessment of mean transit times of tropical montane catchment waters under semi-steady-state conditions, Hydrol. Earth Syst. Sci., 19, 1153-1168, 10.5194/hess-19-1153-2015, 2015.

Tweed, S., Munksgaard, N., Marc, V., Rockett, N., Bass, A., Forsythe, A. J., Bird, M. I., and Leblanc, M.: Continuous monitoring of stream delta O-18 and delta H-2 and stormflow hydrograph separation using laser spectrometry in an agricultural catchment, Hydrol. Process., 30, 648-660, 10.1002/hyp.10689, 2016.

Vitvar, T., and Balderer, W.: Estimation of mean water residence times and runoff generation by O-18 measurements in a pre-Alpine catchment (Rietholzbach, eastern Switzerland), Applied Geochemistry, 12, 787-796, 1997.

Weiler, M., Scherrer, S., Naef, F., and Burlando, P.: Hydrograph separation of runoff components based on measuring hydraulic state variables, tracer experiments, and weighting methods, Integrated Methods in Catchment Hydrology: Tracer, Remote Sensing and New Hydrometric Techniques, 249-255, 1999.

Wels, C., Cornett, R. J., and Lazerte, B. D.: Hydrograph Separation - a Comparison of Geochemical and Isotopic Tracers, Journal of Hydrology, 122, 253-274, 10.1016/0022-1694(91)90181-G, 1991.

Tables

Table 1: Average isotope values and solute concentrations, as well as standard deviations (and relative standard deviations RSD) of three water samples analyzed during two different 48-hour laboratory experiments with the isotope analyzer and IC, respectively. In Fiji bottled water, diluted tap water and nanopure water, concentrations of F^-, Li^+, K^+, NH_4^+ and PO_4^{3-} were mostly below the limit of quantification (LOQ), and thus were not included in the table. The calculation of the average memory coefficient is described in the text (Eq. (1)). The uncertainties of the IC measurements were obtained by simple linear regression analysis of the average value and the standard deviation of the respective constituent.

	Isotope analyzer 48-hour laboratory experiment		IC 48-hour laboratory experiment					
	$\delta^{18}O$	$\delta^{2}H$	Na^+	Mg^{2+}	Ca^{2+}	Cl^-	NO_3^-	SO_4^{2-}
Limit of quantification (LOQ) (mg L^{-1})	-	-	0.1	0.1	0.1	0.05	0.05	0.05
Measurement uncertainty (‰) or (mg L^{-1})	0.03	0.17	0.053+ 0.005·*C*	0.008+ 0.006·*C*	0.087+ 0.009·*C*	0.027+ 0.003·*C*	0.028+ 0.002·*C*	0.037+ 0.006·*C*
Water sample	**Fiji bottled water**		**Fiji bottled water**					
Number of measurements	12	12	10	10	10	10	10	10
Average value (‰) or (mg L^{-1})	-4.86	-35.89	21.6	15.7	24.3	9.69	1.05	1.56
Standard deviation (‰) or (mg L^{-1})	0.06	0.26	0.1	0.1	0.3	0.06	0.05	0.03
RSD (%)	-	-	0.5	0.4	1.1	0.60	4.3	1.80
Linear drift (mean±standard error) ((‰ $24h^{-1}$) or (mg L^{-1} $24h^{-1}$)	-0.009±0.008	0.133±0.040	0.129± 0.056 [a]	0.058± 0.036 [b]	0.093± 0.160 [c]	0.088± 0.019	-0.078± 0.008	0.045± 0.007
Water sample	**Tap water**		**Diluted Ttap water**					
Number of measurements	34	34	17 18	18	18	18	18	18
Average value (‰) or (mg L^{-1})	-9.40	-68.55	10.9	34.4	133.2	12.41	4.96	17.29
Standard deviation (‰) or (mg L^{-1})	0.03	0.12	0.1 2	0.2	1.3	0.057	0.03	0.14
RSD (%)	-	-	0.7 1.6	0.6	1.0	0.5	0.7	0.8
Water sample	**Nanopure water**		**Nanopure water (last sample)**					
Number of measurements	43	43	27	27	27	27	27	27
Average value (‰) or (mg L^{-1})	-9.44	-68.67	<LOQ	0.1	0.6	<LOQ	<LOQ	0.09
Standard deviation (‰) or (mg L^{-1})	0.02	0.18	0.02	0.003	0.1	0.03	0.02	0.05
Carryover (%)	0.9	1.2	2.8	3.3	3.8	2.1	1.9	2.3

[a] $p > 0.05$
[b] $p > 0.15$
[c] $p > 0.50$

Table 2: Characteristics of precipitation events and antecedent moisture conditions during the field experiment. Initial stream stage is used here as a proxy for initial discharge.

~~Event~~	~~Start of event~~	~~Total precipitation (mm)~~	~~Total precipitation until peak flow (mm)~~	~~Response time (h)~~	~~48h antecedent precipitation (mm)~~	~~24h antecedent precipitation (mm)~~	~~Initial stream stage (cm)~~
~~#1~~	~~14 February 2016 10:30~~	~~6.7~~	~~5.1~~	~~01:40~~	~~8.5~~	~~2.9~~	~~0.44~~
~~#2~~	~~20 February 2016 12:30~~	~~10.3~~	~~9.2~~	~~00:00~~	~~1.3~~	~~0.0~~	~~0.36~~
~~#3~~	~~23 February 2016 07:00~~	~~5.0~~	~~4.8~~	~~00:00~~	~~0.2~~	~~0.2~~	~~0.37~~
~~#4~~	~~24 February 2016 15:30~~	~~15.3~~	~~11.1~~	~~01:00~~	~~5.2~~	~~3.3~~	~~0.41~~
~~#5~~	~~28 February 2016 05:50~~	~~10.6~~	~~2.9~~	~~01:10~~	~~0.0~~	~~0.0~~	~~0.38~~
~~#6~~	~~02 March 2016 12:30~~	~~6.0~~	~~6.0~~	~~01:50~~	~~11.9~~	~~2.0~~	~~0.46~~
~~#7~~	~~05 March 2016 05:20~~	~~9.4~~	~~8.6~~	~~01:30~~	~~4.3~~	~~0.9~~	~~0.45~~
~~#8~~	~~07 March 2016 21:00~~	~~6.4~~	~~6.4~~	~~04:00~~	~~1.9~~	~~0.0~~	~~0.45~~

Event	Start of event	Total precipitation (mm)	Total precipitation until peak flow (mm)	Response time (h:min)	48h antecedent precipitation (mm)	24h antecedent precipitation (mm)	Initial stream stage (m)
#1	14 February 2016 11:00	5.8	2.2	01:10	8.3	2.7	0.44
#2	20 February 2016 10:00	11.5	8.8	00:30	1.9	0.5	0.36
#3	23 February 2016 8:00	5.8	3.5	00:00	0.8	0.8	0.37
#4	24 February 2016 15:00	14.3	8.1	01:00	6.6	5.0	0.41
#5	29 February 2016 13:00	10.5	2.0	00:00	0.0	0.0	0.38
#6	2 March 2016 13:00	8.7	6.8	01:10	12.3	1.9	0.46
#7	5 March 2016 4:00	11.5	9.4	02:10	4.6	0.9	0.45
#8	7 March 2016 23:00	8.4	8.4	02:30	0.6	0.0	0.45

Figures

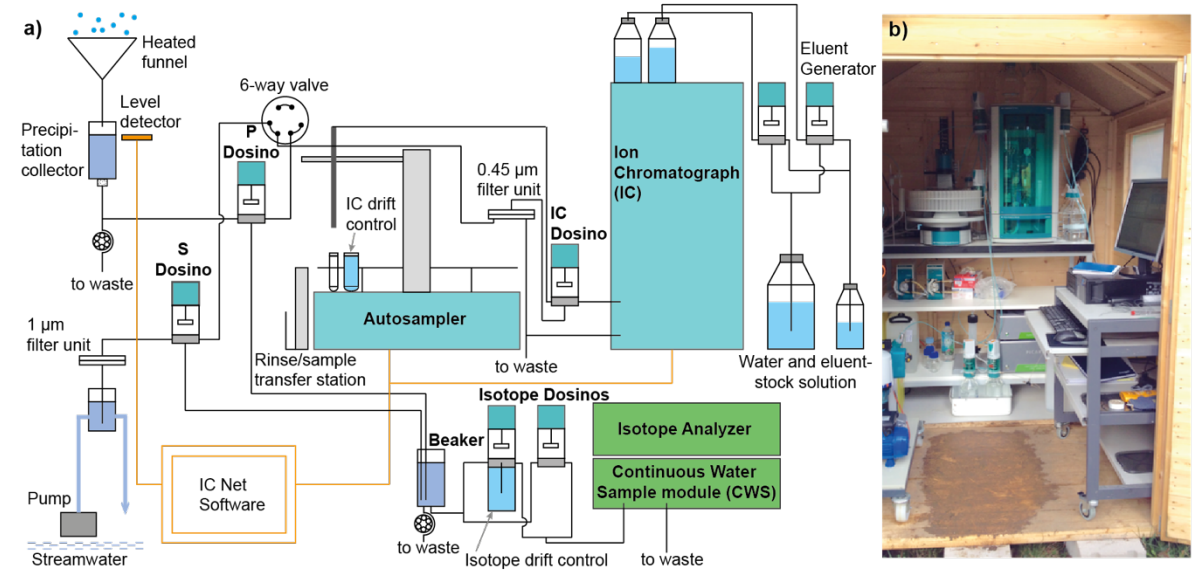

Figure 1: a) Schematic overview of the coupled isotope analyzer / IC- system for the collection and ~~measurement~~ analysis of streamwater and precipitation samples. Components of the sample distribution and the IC are shown in blue ~~color~~, while the isotope analyzer with CWS is shown in green ~~color~~. Panel b) shows a photo of the coupled isotope analyzer / IC- system in the wooden hut during the field experiment.

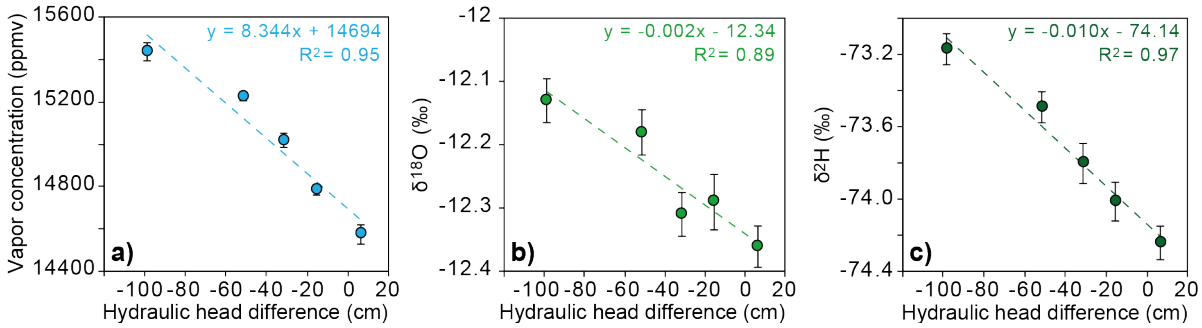

Figure 2: Experiment showing the isotope effects of sample injection into the continuous water sampler (CWS). Panel a) shows m~~M~~easured vapor concentrations, and (panels ba) and c), show the ~~and~~ raw, uncalibrated isotope ~~ratios~~ values ~~(panels b) and c))~~ of a single water sample (nanopure water) as a function of the hydraulic head difference between the water level in the sample bottle and the waste outlet. Negative values of the hydraulic head difference indicate that the sample source was located below the waste outlet of the CWS.

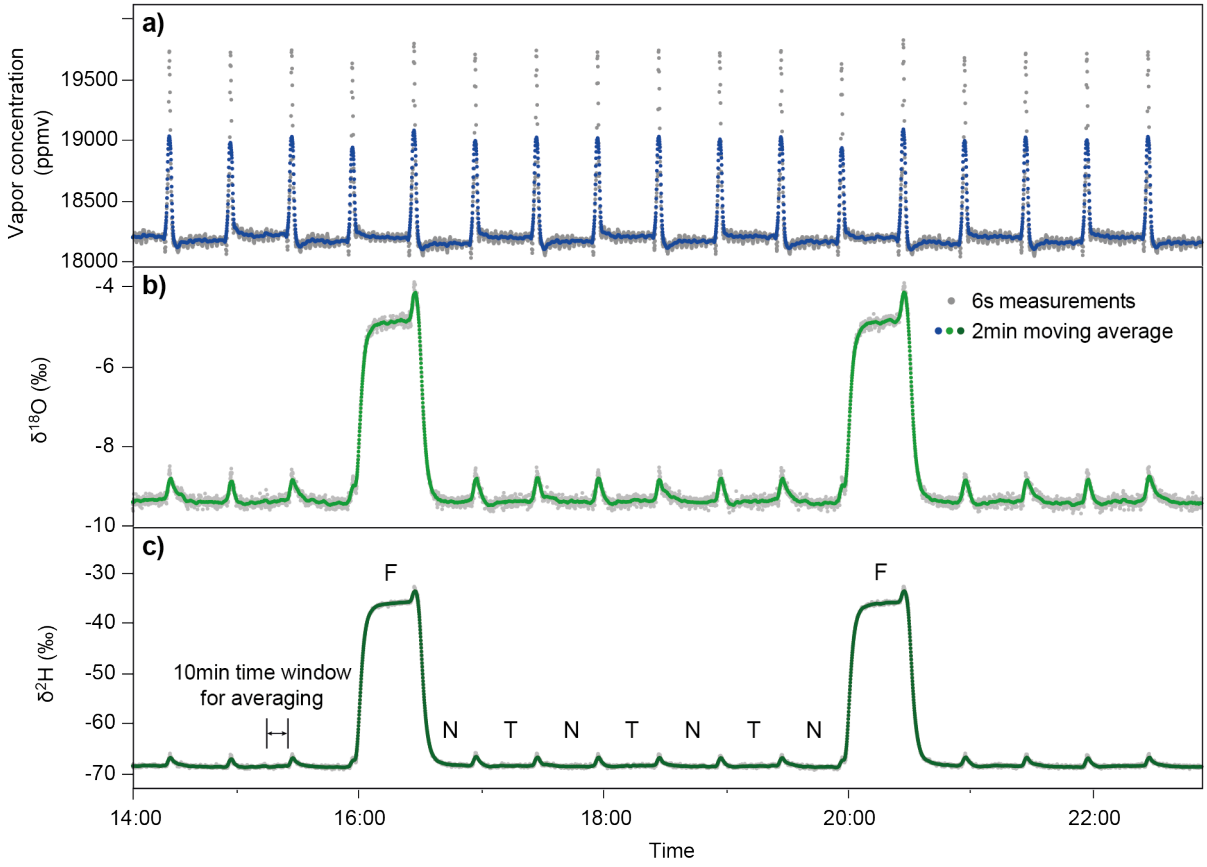

Figure 3: ~~Nine hour~~Nine-hour excerpt showing raw, uncalibrated data of vapor concentrations (panel a)) and isotope measurements (panels b) and c)) in tap water (T), nanopure water (N) and Fiji bottled water (F) during the 48-hour laboratory experiment. Samples were injected alternately with two Dosinos for 30min each at a flow rate of 1 mL min^{-1}.

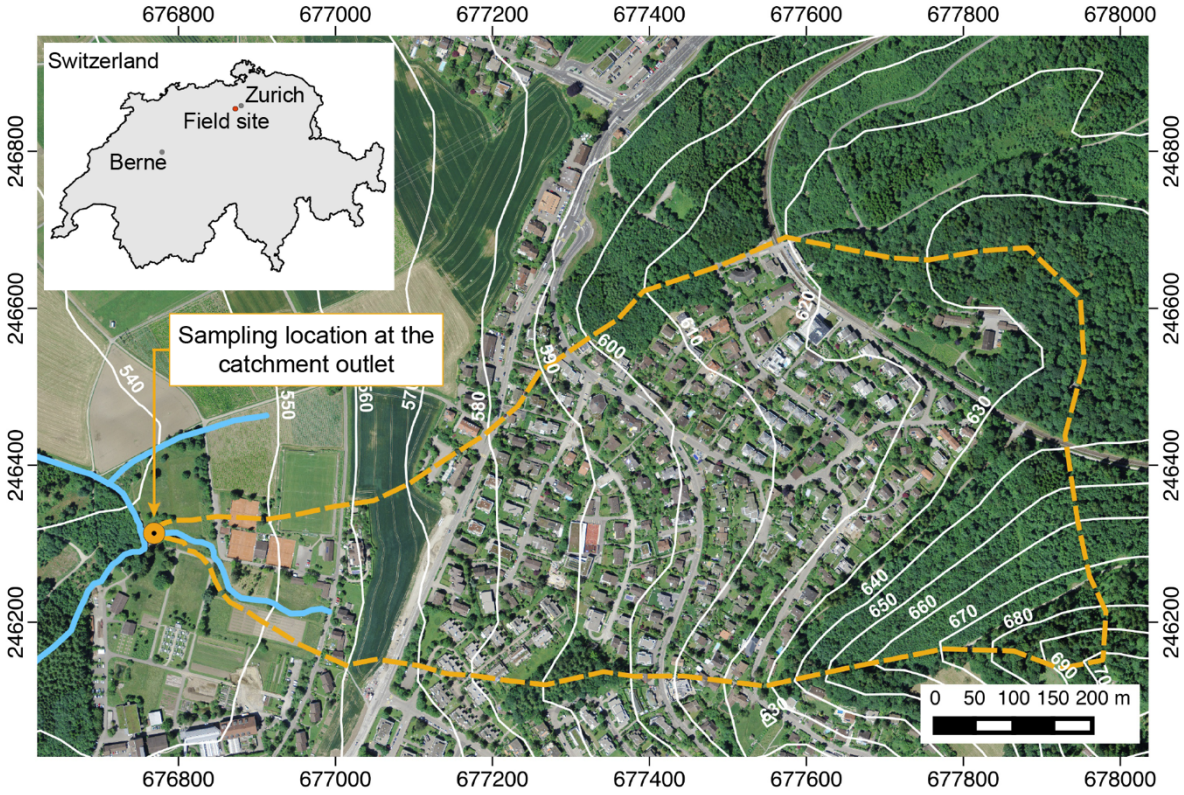

Figure 4: Location of the field site at a small creek on the property of the Swiss Federal Institute for Forest, Snow and Landscape Research (WSL) near Zurich, Switzerland. Catchment boundaries are approximate.

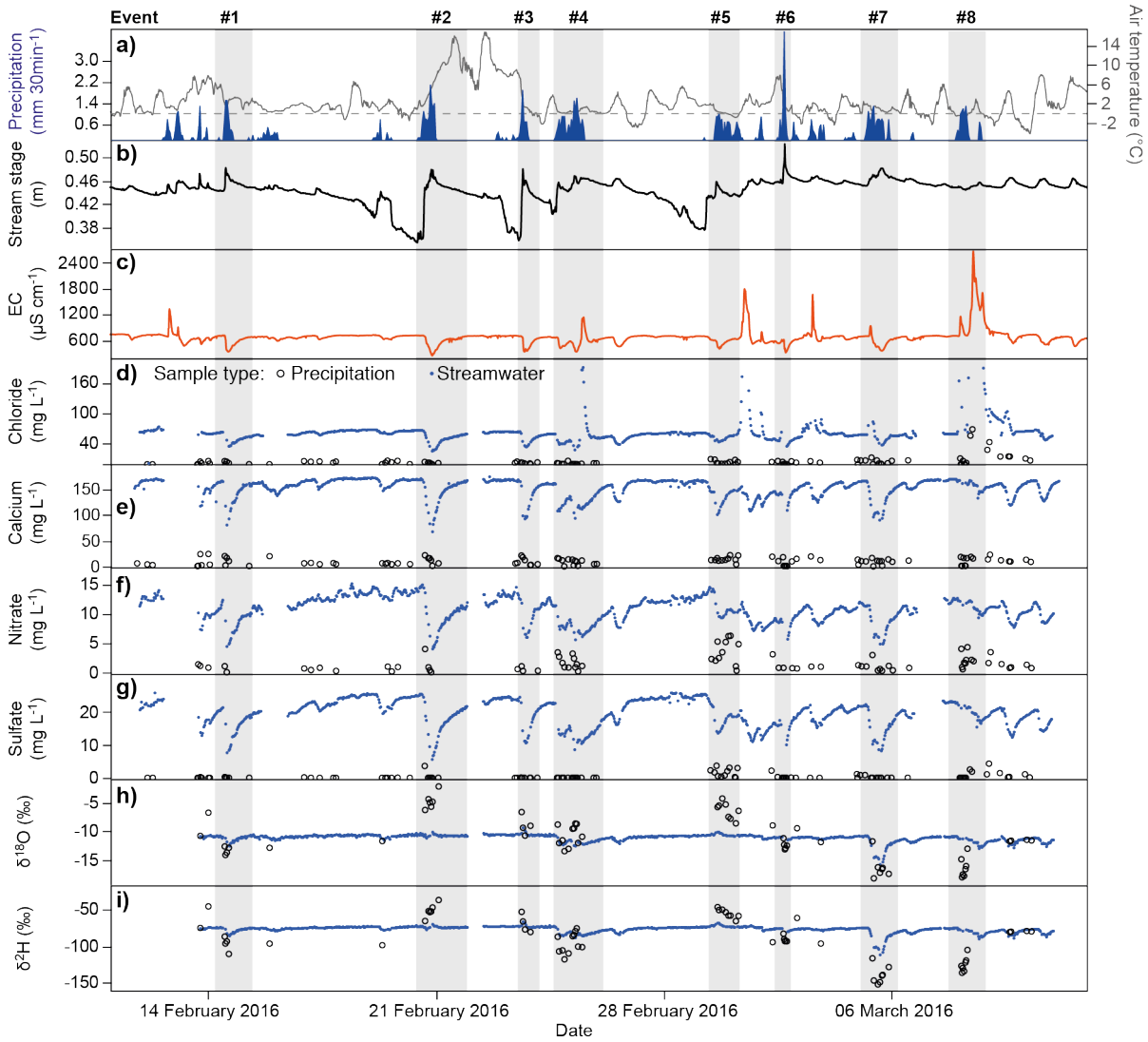

Figure 5: Time series of a) precipitation and, air temperature, as well as (ba) and stream stage (b) at the field site during the four-week study period. Panels c) and d) shows streamwater EC the chloride and nitrate concentrations, whereas panels d – g) show the chloride, calcium, nitrate and sulfate concentrations, respectively. Panels he) and if) show the isotopic compositions of precipitation and streamwater samples. Streamwater samples are shown by blue dots and precipitation samples are shown by open circles. Vertical grey bars indicate the periods of the eight precipitation events used for hydrograph separation.

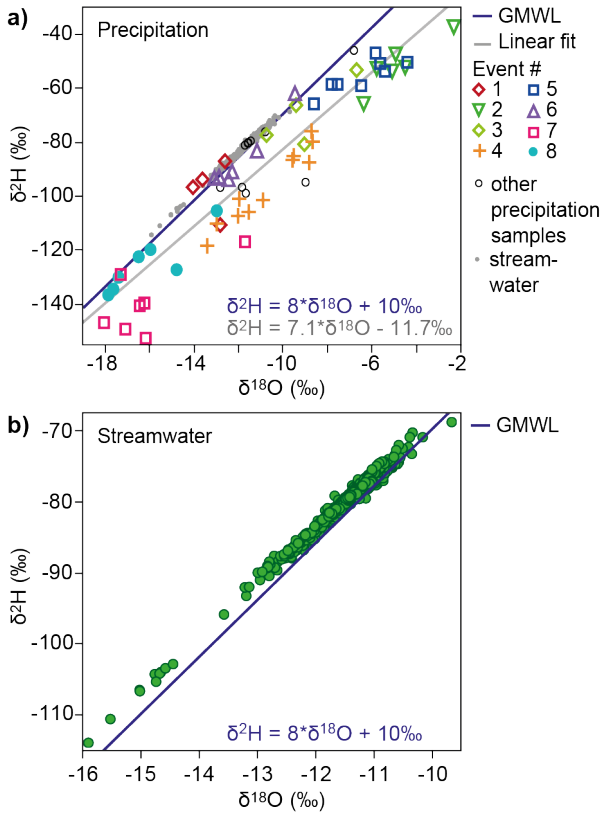

Figure 6: Dual-isotope plot of all $\delta^{18}O$ and $\delta^{2}H$ values measured in a) precipitation ~~(a)~~ and b) streamwater ~~(b)~~ during the field experiment. Streamwater samples are also plotted in grey in the upper panel for comparison (note the difference in scales). The global meteoric water line (GWML, Craig (1961)) and the linear fit to the precipitation data ~~(local meteoric water line, LMWL)~~ are shown in blue and in grey, respectively.

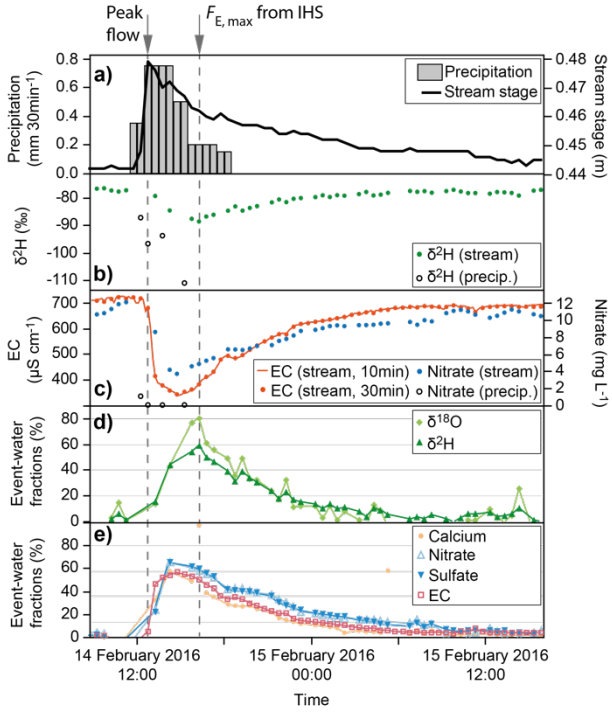

Figure 7: Precipitation Event #1 together with the a) hydrologic ~~(a)~~, b) isotopic ~~(b)~~ and c) chemical ~~(c)~~ responses in streamwater. Panels d) and e) show the fractions of event-water based on isotopic and chemical hydrograph separation, respectively, which are similar for both types of tracers. However, the timing of the maximum event-water fraction ($F_{E,max}$) differs, withi~~.e.~~ the isotopes indicatinge the largest contribution of event water around 32h after the ~~flood~~ peak flow(Q_{max}) was reached. In panel e), gaps in the F_E time series based on calcium concentrations are due to measurement outliers.

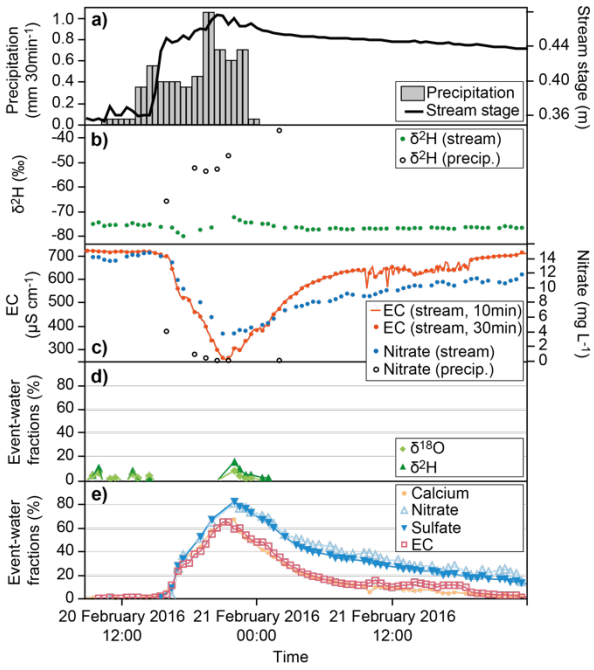

Figure 8: Precipitation Event #2 and the a) hydrologic, b) isotopic and c) chemical responses in streamwater. Panels d) and e) show the fractions of event water (F_E) based on isotopic and chemical hydrograph separation. Chemical tracers greatly exaggerate the event-water fraction.

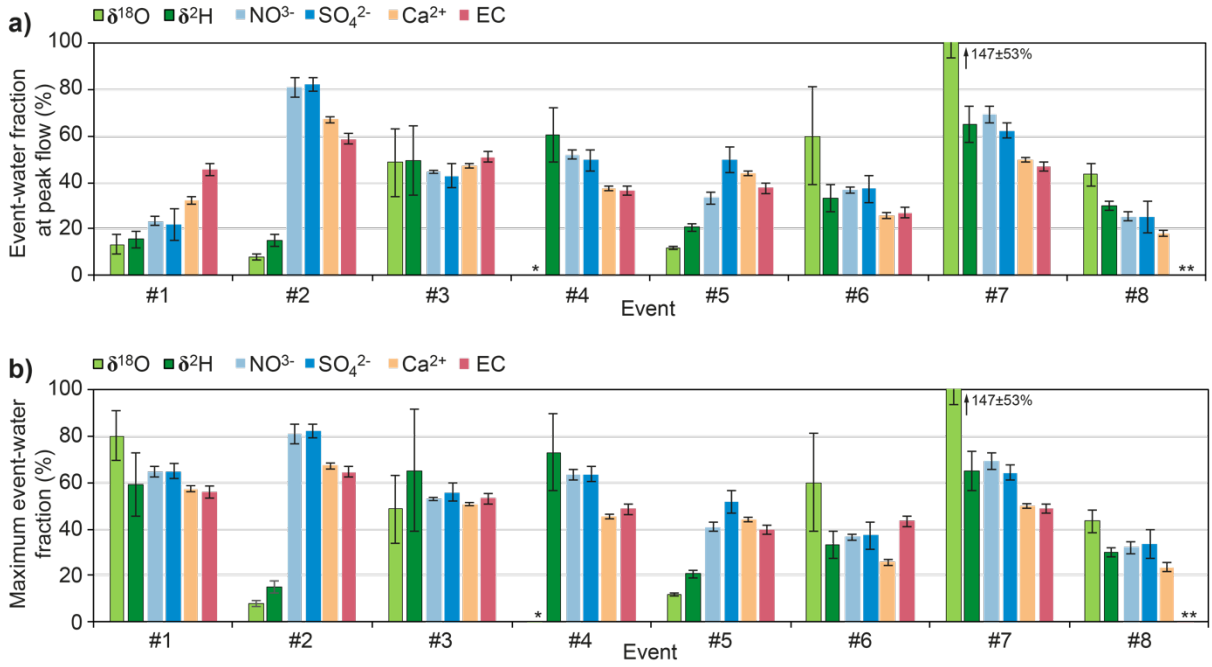

Figure 9: Event-water fractions (F_E) based on isotopic and chemical hydrograph separation for eight storm events. Panel a) shows F_E during peak flow, and panel b) shows the maximum event-water fractions ($F_{E,max}$) of each event. Unrealistic F_E and $F_{E,max}$ values based on $\delta^{18}O$ were obtained for Event #4 ~~based on $\delta^{18}O$~~ because the isotopic signatures in precipitation and pre-event streamwater were too similar (*). For Event #8, wash-off of road salt resulted in unrealistic F_E and $F_{E,max}$ values based on EC, i.e. -96±6% and -95±~~7~~6% (**), respectively. The larger uncertainties of the IHS results compared to CHS can be explained with the large temporal variability of the isotope values in precipitation, which substantially exceeds analytical uncertainty during most events.

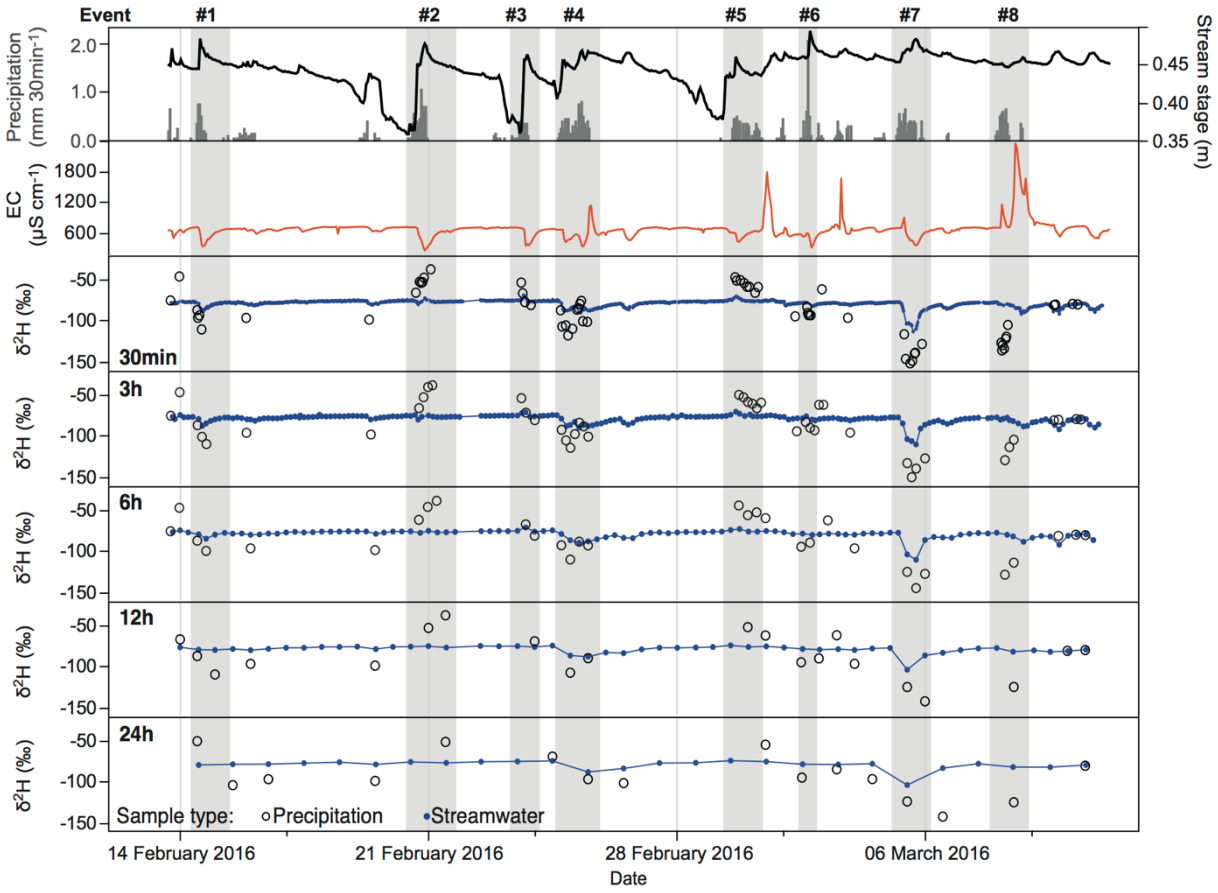

Figure 10: Time series of precipitation, stream stage and streamwater EC, ~~(at 10min temporal resolution),~~ as well as δ^2H values in streamwater and precipitation at sampling intervals of 30 min, 3 h, 6 h, 12 h and 24 h. Streamwater isotope values at 3 h – 24 h temporal resolution were obtained by sub-sampling from the 30 min time series. To mimic the effects of integrated bulk precipitation samples, isotope values in precipitation were calculated from volume-weighted averaging the 30 min data over the corresponding time intervals. Vertical grey bars indicate the periods of the eight precipitation events used for hydrograph separation.

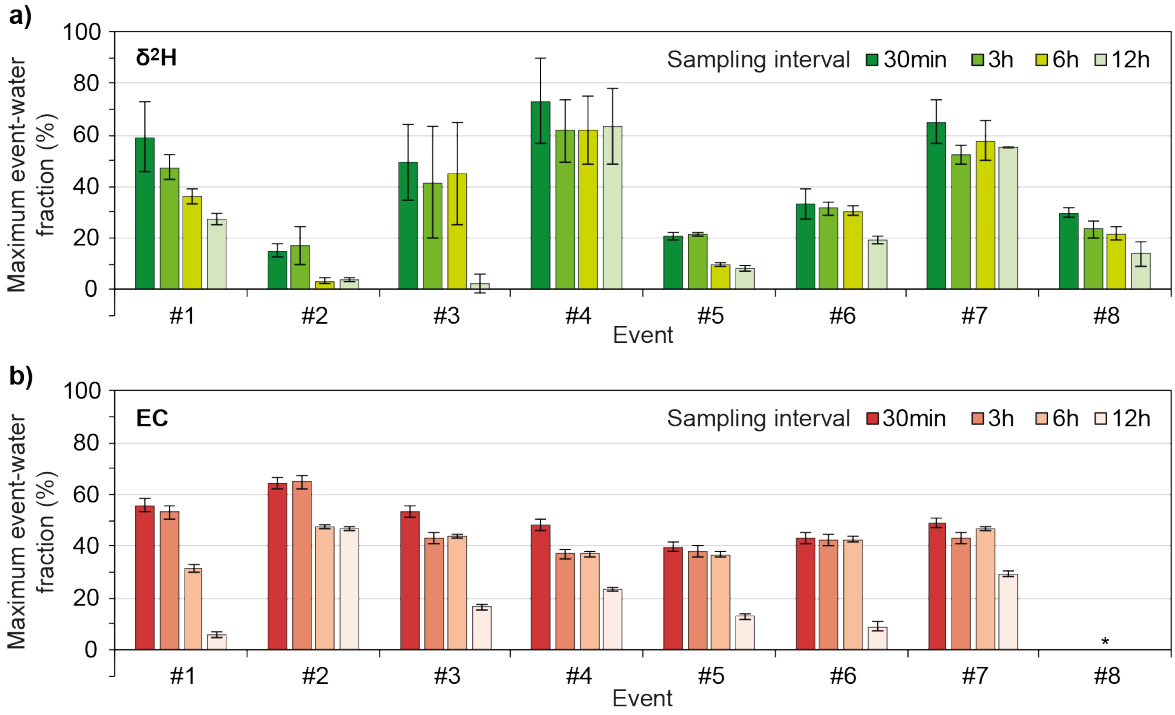

Figure 11: ~~MEvent-water fractions at peak flow (a) and m~~**aximum event-water fractions** ~~(b)~~ **at sampling intervals of 30 min, 3 h, 6 h and 12 h based on a) δ^2H and b) EC.** ~~measurements at sampling intervals of 30min, 3h, 6h and 12h.~~ **With lower sampling frequencies, the event-water fractions are often underestimated or become even unrealistic, as the likelihood increases that the point of largest δ^2H or EC variations in streamflow will be missed (**~~,~~**Streamwater δ^2H and EC time series were subsampled at 3-hourly, 6-hourly, 12-hourly and daily intervals; concentrations of integrated bulk precipitation samples were calculated from the volume-weighted averages over the respective time interval. For Event #8, wash-off of road salt resulted in unrealistic $F_{E,max}$ values based on EC (*).).**

A lab in the field: High-frequency analysis of water quality and stable isotopes in streamwater and precipitation

Jana von Freyberg[1, 2], Bjørn Studer[1], James W. Kirchner[1, 2]

[1] Department of Environmental Systems Science, ETH Zurich, Zurich, Switzerland

[2] Swiss Federal Research Institute WSL, Birmensdorf, Switzerland

Correspondence to: Jana von Freyberg (jana.vonfreyberg@usys.ethz.ch)

Supplement

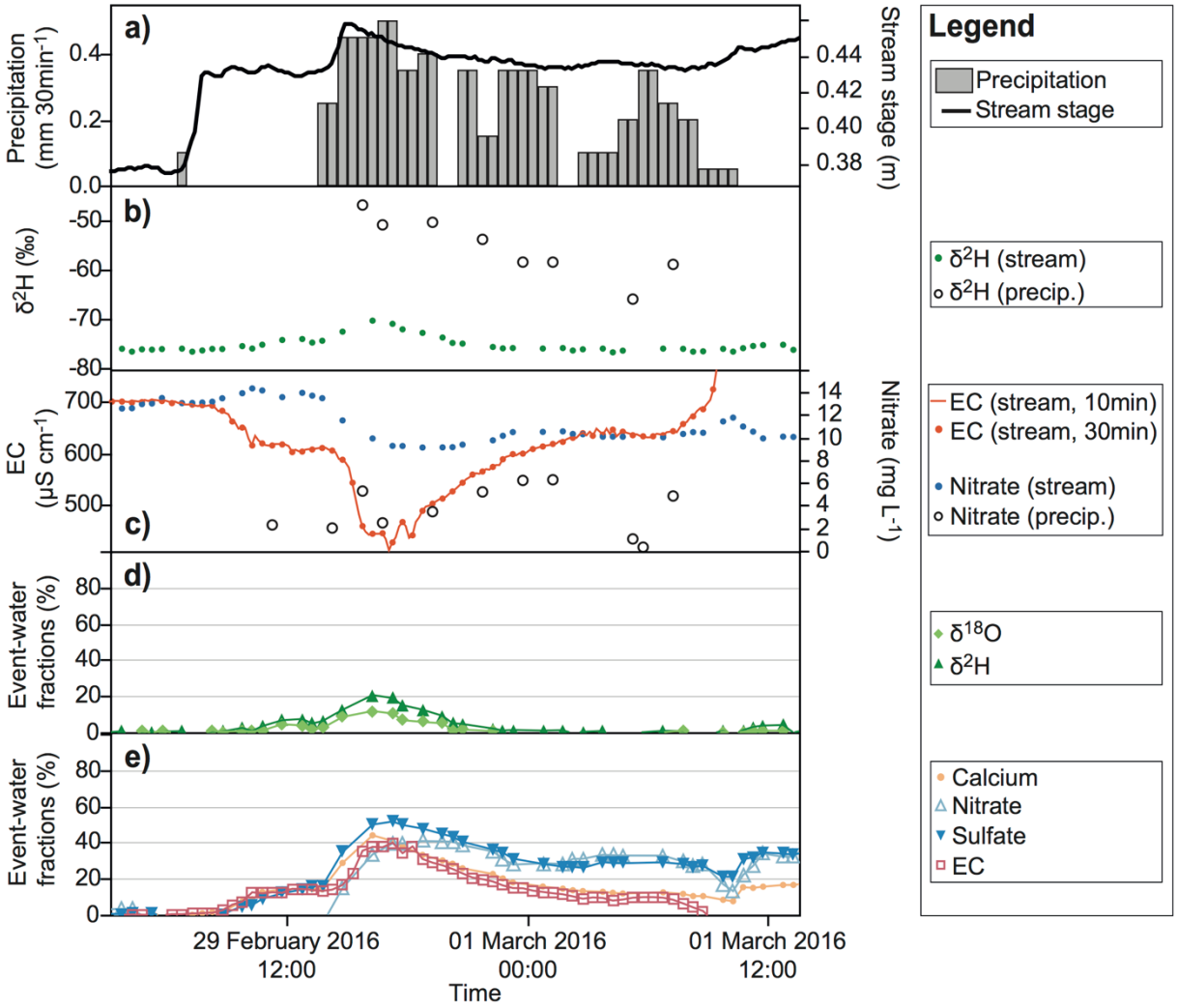

Figure S1: Precipitation Event #5 together with the hydrologic ~~(~~a), isotopic ~~(~~b) and chemical ~~(~~c) responses in streamwater. Panels d) and e) show the fractions of event-water based on isotopic hydrograph separation ~~(IHS)~~ and chemical hydrograph separation ~~(CHS)~~, respectively, which are different for both types of tracers: While the ~~IHS~~ isotope tracers yields event-water fractions smaller than 2~~1~~0%, ~~CHS based on~~ chemical tracers estimated much larger event-water fractions of more than 40%.

Table S 1: End-members and event-water fractions during peak flow.

-	$\delta^{18}O$ (‰)	$\delta^{2}H$ (‰)	Ca^{2+} (mg L^{-1})	NO_3^- (mg L^{-1})	SO_4^{2-} (mg L^{-1})	EC (µS cm^{-1})
Event	**Pre-event-water end member (C_P) ±SE_{CP}**					
#1	-11.16±0.08	-77.22±0.29	162.68±1.60	11.04±0.24	20.06±1.25	710.20±14.57
#2	-10.81±0.07	-75.50±0.29	166.58±1.59	13.62±0.15	23.98±1.48	718.00±14.38
#3	-10.85±0.03	-75.55±0.18	166.28±1.62	12.84±0.10	23.77±1.47	712.20±14.27
#4	-10.92±0.06	-75.78±0.34	158.00±1.52	11.53±0.21	21.95±1.36	669.80±13.92
#5	-10.93±0.03	-76.26±0.20	163.97±1.66	12.94±0.18	24.46±1.51	700.60±14.02
#6	-11.36±0.05	-79.13±0.26	142.07±1.56	8.50±0.15	15.20±0.99	586.00±12.15
#7	-11.09±0.03	-77.61±0.18	163.61±1.57	11.52±0.12	21.05±1.30	695.80±13.99
#8	-11.16±0.03	-77.96±0.19	167.56±1.59	12.14±0.16	22.34±1.38	708.60±14.23
Event	**Event-water end member (C_E) ±SE_{CE} at peak flow**					
#1	-13.21±0.36	-91.34±2.34	14.78±4.32	0.55±0.28	0.16±0.08	64.28±26.86
#2	-5.25±0.41	-55.01±3.16	14.55±2.74	1.41±0.64	1.07±0.60	14.05±20.65
#3	-8.37±0.74	-62.05±4.08	17.35±1.26	0.48±0.13	0.07±0.04	26.41±20.29
#4	-10.99±0.55	-98.84±4.37	9.26±1.87	1.94±0.30	0.05±0.04	4.94±20.04
#5	-5.78±0.10	-47.64±1.58	14.36±1.05	3.95±0.63	2.60±0.66	12.04±20.08
#6	-12.04±0.23	-88.96±1.54	6.03±2.04	0.27±0.09	0.05±0.04	8.90±20.29
#7	-14.36±1.19	-133.59±7.28	11.75±2.16	1.52±0.50	0.09±0.05	21.99±21.07
#8	-15.87±0.53	-125.34±3.00	10.48±2.39	2.46±0.39	0.18±0.14	17.35±20.79
Event	**Streamwater end member (C_S) ±SE_{CS} at peak flow**					
#1	-11.43±0.03	-79.39±0.17	114.90±1.11	8.60±0.04	15.72±0.98	414.00±8.28
#2	-10.39±0.03	-72.41±0.17	64.60±0.66	3.73±0.03	5.12±0.34	304.00±6.08
#3	-9.65±0.03	-68.88±0.17	96.38±0.94	7.36±0.04	13.63±0.85	363.00±7.26
#4	-12.65±0.03	-89.72±0.17	101.97±0.99	6.56±0.04	11.10±0.70	428.00±8.56
#5	-10.32±0.03	-70.36±0.17	98.23±0.96	9.94±0.04	13.56±0.85	442.00±8.84
#6	-11.77±0.03	-82.40±0.17	107.28±1.04	5.48±0.04	9.57±0.61	431.00±8.62
#7	-15.89±0.03	-113.99±0.17	88.22±0.87	4.62±0.04	7.98±0.52	380.00±7.60
#8	-13.20±0.03	-92.12±0.17	139.13±1.33	9.68±0.04	16.80±1.05	1369.00±27.38

	Event-water fraction F_E ±SE (%) at peak flow					
Event	**$\delta^{18}O$**	**$\delta^{2}H$**	**Ca^{2+}**	**NO_3^-**	**SO_4^{2-}**	**EC**
#1	13.36±4.28	15.40±3.33	32.31±1.41	23.30±1.89	21.84±6.95	45.86±2.60
#2	7.64±1.33	15.09±2.75	67.08±1.33	80.98±4.28	82.33±2.87	58.81±2.10
#3	48.66±14.64	49.36±14.99	46.94±0.95	44.30±0.72	42.77±5.05	50.92±2.11
#4	-[a]	60.45±11.50	37.67±1.04	51.86±1.99	49.53±4.48	36.37±2.15
#5	11.77±0.82	20.59±1.40	43.94±0.95	33.39±2.72	49.87±5.42	37.56±2.11
#6	60.14±21.00	33.30±5.78	25.58±1.21	36.73±1.33	37.19±5.75	26.86±2.34
#7	146.70±53.19	64.98±8.46	49.64±1.05	69.04±3.48	62.36±3.40	46.87±2.15
#8	43.49±4.97	29.89±1.95	18.10±1.21	25.40±1.64	24.98±6.64	-95.54±6.34[b]

-	~~$\delta^{18}O$ (‰)~~	~~$\delta^{2}H$ (‰)~~	~~Ca^{2+} (mg L^{-1})~~	~~NO_3^- (mg L^{-1})~~	~~SO_4^{2-} (mg L^{-1})~~	~~EC (µS cm^{-1})~~
~~**Event**~~	~~**Pre-event-water end member (C_P) ±SE_{CP}**~~					
~~#1~~	~~-10.98±0.03~~	~~-75.10±0.20~~	~~162.84±1.84~~	~~11.33±0.05~~	~~20.22±1.27~~	~~708.80±18.45~~
~~#2~~	~~-10.61±0.07~~	~~-73.36±0.29~~	~~166.66±1.58~~	~~13.85±0.12~~	~~24.18±1.49~~	~~718.40±14.39~~

#3	-10.71±0.03	-73.57±0.18	166.28±1.62	12.84±0.10	23.77±1.47	711.20±14.28
#4	-10.77±0.05	-73.74±0.32	158.11±1.53	11.18±0.08	21.84±1.35	667.00±13.88
#5	-10.78±0.03	-74.24±0.20	163.97±1.66	12.94±0.18	24.46±1.51	700.40±14.01
#6	-11.25±0.03	-77.30±0.21	137.90±1.86	8.05±0.10	14.23±0.92	562.20±12.61
#7	-10.93±0.03	-75.52±0.18	163.61±1.57	11.52±0.12	21.05±1.30	694.40±13.93
#8	-11.06±0.04	-76.20±0.21	166.67±1.61	11.66±0.10	22.22±1.37	696.80±14.09
Event	Event water end member (C_E) ±SE_{CE} at peak flow					
#1	-13.00±0.26	-91.86±3.65	13.14±3.19	0.38±0.22	0.12±0.06	53.88±24.97
#2	-5.62±0.30	-55.71±2.57	15.90±2.37	1.63±0.66	1.27±0.63	15.80±20.69
#3	-8.42±0.73	-61.52±4.44	16.31±0.89	0.46±0.13	0.07±0.04	24.02±20.34
#4	-10.70±0.54	-94.29±4.36	10.05±1.69	1.84±0.30	0.05±0.04	5.91±20.07
#5	-5.92±0.09	-46.96±1.32	13.76±1.01	3.39±0.71	2.39±0.60	12.87±20.07
#6	-11.87±0.40	-86.22±2.21	6.99±3.76	0.31±0.16	0.05±0.04	10.58±20.92
#7	-14.58±1.06	-130.11±6.16	10.81±2.21	1.28±0.50	0.06±0.04	18.15±21.15
#8	-15.29±0.50	-121.41±2.76	12.15±2.56	2.72±0.45	0.17±0.15	20.24±20.98
Event	Streamwater end member (C_S) ±SE_{CS} at peak flow					
#1	-11.85±0.03	-82.19±0.17	78.00±0.78	4.16±0.03	7.12±0.46	414.00±8.28
#2	-10.27±0.03	-70.60±0.17	64.60±0.66	3.73±0.03	5.12±0.34	264.00±5.28
#3	-10.04±0.03	-69.28±0.17	89.92±0.89	6.26±0.04	10.52±0.67	346.00±6.92
#4	-12.54±0.03	-87.74±0.17	90.82±0.90	5.39±0.04	8.00±0.52	428.00±8.56
#5	-10.20±0.03	-68.66±0.17	98.23±0.96	9.94±0.04	13.56±0.85	542.00±10.84
#6	-11.58±0.03	-80.06±0.17	107.28±1.04	5.48±0.04	9.57±0.61	336.00±7.24
#7	-15.12±0.03	-106.78±0.17	91.31±0.90	4.58±0.04	7.59±0.49	366.00±7.32
#8	-12.54±0.03	-85.85±0.17	142.95±1.36	9.65±0.04	16.71±1.04	1338.00±26.76

	Event water fraction F_E ±SE (%) at peak flow					
Event	$\delta^{18}O$	$\delta^{2}H$	Ca^{2+}	NO_3^-	SO_4^{2-}	EC
#1	42.85±5.80	42.29±9.28	56.67±1.42	65.45±1.35	65.21±3.20	45.01±2.64
#2	6.72±1.49	15.68±2.84	67.70±1.20	82.84±4.50	83.17±2.95	64.67±2.17
#3	29.21±9.43	35.61±13.23	50.92±0.85	53.15±0.75	55.93±3.92	53.15±2.11
#4	-[a]	68.15±14.48	45.45±0.98	61.99±2.06	63.53±3.28	36.15±2.16
#5	11.79±0.85	20.44±1.30	43.77±0.94	31.43±2.69	49.40±5.35	23.04±2.32
#6	52.06±34.19	30.90±8.05	23.39±1.51	33.24±1.24	32.92±6.13	36.29±2.40
#7	114.79±33.35	57.27±6.47	47.32±1.05	67.77±3.34	64.11±3.24	48.56±2.15
#8	35.03±4.22	21.36±1.40	15.35±1.27	22.44±1.49	25.02±6.63	-94.77±6.38[b]

[a] Unrealistic event-water fractions were obtained because the $\delta^{18}O$ signatures in precipitation and streamwater were too similar.

[b] Wash-off of road salt resulted in unrealistic event-water fractions based on EC.

Table S 2: End-members and event-water fractions during maximum event-water fraction.

-	$\delta^{18}O$ (‰)	$\delta^{2}H$ (‰)	Ca^{2+} (mg L^{-1})	NO_3^- (mg L^{-1})	SO_4^{2-} (mg L^{-1})	EC (µS cm^{-1})
Event	**Pre-event-water end member (C_P) ±SE_{CP}**					
#1	-11.16±0.08	-77.22±0.29	162.68±1.60	11.04±0.24	20.06±1.25	710.20±14.57
#2	-10.81±0.07	-75.50±0.29	166.58±1.59	13.62±0.15	23.98±1.48	718.00±14.38
#3	-10.85±0.03	-75.55±0.18	166.28±1.62	12.84±0.10	23.77±1.47	712.20±14.27
#4	-10.92±0.06	-75.78±0.34	158.00±1.52	11.53±0.21	21.95±1.36	669.80±13.92
#5	-10.93±0.03	-76.26±0.20	163.97±1.66	12.94±0.18	24.46±1.51	700.60±14.02
#6	-11.36±0.05	-79.13±0.26	142.07±1.56	8.50±0.15	15.20±0.99	586.00±12.15
#7	-11.09±0.03	-77.61±0.18	163.61±1.57	11.52±0.12	21.05±1.30	695.80±13.99
#8	-11.16±0.03	-77.96±0.19	167.56±1.59	12.14±0.16	22.34±1.38	708.60±14.23
Event	**Event-water end member (C_E) ±SE_{CE} at maximum event-water fraction**					
#1	-13.17±0.27	-96.54±4.42	14.65±3.07	0.4±0.23	0.13±0.07	55.09±25.08
#2	-5.25±0.41	-55.01±3.16	14.55±2.74	1.41±0.64	1.07±0.60	15.57±20.81
#3	-8.37±0.74	-62.05±4.08	15.6±1.30	0.39±0.14	0.07±0.04	24.86±20.47
#4	-10.68±0.55	-95.95±4.56	9.36±1.65	1.84±0.29	0.05±0.04	4.15±20.03
#5	-5.78±0.10	-47.64±1.58	14.36±1.05	3.6±0.34	1.97±0.60	9.17±20.07
#6	-12.04±0.23	-88.96±1.54	6.03±2.04	0.27±0.09	0.05±0.04	9.01±20.29
#7	-14.36±1.19	-133.59±7.28	11.75±2.16	1.52±0.50	0.08±0.05	19.68±21.12
#8	-15.87±0.53	-125.34±3.00	10.35±9.73	2.5±0.68	0.15±1.19	16.53±20.79
Event	**Streamwater end member (C_S) ±SE_{CS} at maximum event-water fraction**					
#1	-12.77±0.03	-88.67±0.17	78.00±0.78	4.16±0.15	7.12±0.46	343.00±7.16
#2	-10.39±0.03	-72.41±0.17	64.60±0.66	3.73±0.03	5.12±0.34	264.00±5.28
#3	-9.65±0.03	-68.88±0.17	89.92±0.89	6.26±0.04	10.52±0.67	346.00±6.92
#4	-12.78±0.03	-90.53±0.17	90.82±0.90	5.39±0.04	8.00±0.52	347.00±6.94
#5	-10.32±0.03	-70.36±0.17	98.23±0.96	9.13±0.04	12.86±0.81	425.00±8.50
#6	-11.77±0.03	-82.40±0.17	107.28±1.04	5.48±0.04	9.57±0.61	336.00±6.72
#7	-15.89±0.03	-113.99±0.17	88.22±0.87	4.62±0.04	7.59±0.49	366.00±7.32
#8	-13.20±0.03	-92.12±0.17	130.86±1.25	9.06±0.04	14.83±0.93	1369.00±27.38

	Maximum event-water fraction $F_{E,max}$ ±SE_{FE} (%)					
Event	**$\delta^{18}O$**	**$\delta^{2}H$**	**Ca^{2+}**	**NO_3^-**	**SO_4^{2-}**	**EC**
#1	80.21±10.75	59.28±13.61	57.20±1.38	64.63±2.14	64.95±3.21	56.05±2.60
#2	7.64±1.33	15.09±2.75	67.08±1.33	80.98±4.28	82.33±2.87	64.63±2.18
#3	48.66±14.64	49.36±14.99	50.68±0.91	52.85±0.76	55.91±3.92	53.28±2.11
#4	-[a]	73.11±16.55	45.20±0.96	63.32±2.07	63.72±3.26	48.49±2.09
#5	11.77±0.82	20.59±1.4	43.94±0.95	40.74±1.91	51.58±5.03	39.86±2.08
#6	60.14±21.00	33.30±5.78	25.58±1.21	36.73±1.33	37.19±5.75	43.33±2.26
#7	146.70±53.19	64.98±8.46	49.64±1.05	69.04±3.48	64.18±3.24	48.78±2.15
#8	43.49±4.97	29.89±1.95	23.34±1.82	31.95±2.55	33.82±6.13	-95.42±6.33[b]

~~-~~	~~$\delta^{18}O$ (‰)~~	~~$\delta^{2}H$ (‰)~~	~~Ca^{2+} (mg L^{-1})~~	~~NO_3^- (mg L^{-1})~~	~~SO_4^{2-} (mg L^{-1})~~	~~EC (µS cm^{-1})~~
~~**Event**~~	~~**Pre-event-water end member (C_P) ±SE_{CP}**~~					
~~#1~~	~~-10.98±0.03~~	~~-75.10±0.20~~	~~162.84±1.84~~	~~11.33±0.05~~	~~20.22±1.27~~	~~708.80±18.45~~
~~#2~~	~~-10.61±0.07~~	~~-73.36±0.29~~	~~166.66±1.58~~	~~13.85±0.12~~	~~24.18±1.49~~	~~718.40±14.39~~
~~#3~~	~~-10.71±0.03~~	~~-73.57±0.18~~	~~166.28±1.62~~	~~12.84±0.10~~	~~23.77±1.47~~	~~711.20±14.28~~
~~#4~~	~~-10.77±0.05~~	~~-73.74±0.32~~	~~158.11±1.53~~	~~11.18±0.08~~	~~21.84±1.35~~	~~667.00±13.88~~
~~#5~~	~~-10.78±0.03~~	~~-74.24±0.20~~	~~163.97±1.66~~	~~12.94±0.18~~	~~24.46±1.51~~	~~700.40±14.01~~
~~#6~~	~~-11.25±0.03~~	~~-77.30±0.21~~	~~137.90±1.86~~	~~8.05±0.10~~	~~14.23±0.92~~	~~562.20±12.61~~

#7	-10.93±0.03	-75.52±0.18	163.61±1.57	11.52±0.12	21.05±1.30	694.40±13.93
#8	-11.06±0.04	-76.20±0.21	166.67±1.61	11.66±0.10	22.22±1.37	696.80±14.09
Event	Event-water end member (C_E) ±SE_{CE} at maximum event-water fraction					
#1	-12.95±0.25	-93.36±4.23	13.14±3.19	0.38±0.22	0.12±0.06	50.64±24.97
#2	-5.62±0.30	-55.71±2.57	15.90±2.37	1.63±0.66	1.27±0.63	15.80±20.69
#3	-7.99±0.90	-58.77±4.26	16.31±0.89	0.46±0.13	0.07±0.04	24.02±20.34
#4	-10.70±0.54	-94.29±4.36	10.05±1.69	1.84±0.30	0.05±0.04	5.47±20.06
#5	-5.92±0.09	-46.96±1.32	13.76±1.01	3.51±0.46	2.08±0.56	10.58±20.09
#6	-11.87±0.40	-86.22±2.21	6.99±3.76	0.31±0.16	0.05±0.04	10.58±20.92
#7	-14.24±1.28	-129.38±7.76	11.53±2.41	1.49±0.56	0.06±0.04	18.15±21.17
#8	-15.29±0.50	-121.41±2.76	12.07±2.62	2.77±0.45	0.13±0.14	20.24±20.98
Event	Streamwater end member (C_S) ±SE_{CS} at maximum event-water fraction					
#1	-12.52±0.03	-85.99±0.17	78.00±0.78	4.16±0.15	7.12±0.46	343.00±6.86
#2	-10.27±0.03	-70.60±0.17	64.60±0.66	3.73±0.03	5.12±0.34	264.00±5.28
#3	-9.57±0.03	-67.26±0.17	89.92±0.89	5.77±0.04	10.03±0.67	346.00±6.92
#4	-12.54±0.03	-87.74±0.17	90.82±0.90	5.39±0.04	8.00±0.52	347.00±6.94
#5	-10.20±0.03	-68.66±0.17	98.23±0.96	9.13±0.04	12.86±0.81	425.00±8.50
#6	-11.58±0.03	-80.06±0.17	107.28±1.04	5.48±0.04	9.57±0.61	336.00±6.72
#7	-15.48±0.03	-109.94±0.17	88.22±0.87	4.58±0.04	7.59±0.49	366.00±7.32
#8	-12.93±0.03	-89.25±0.17	130.86±1.25	9.06±0.04	14.83±0.93	1577.00±26.76

	Maximum event-water fraction $F_{E,max}$ ±SE_{FE} (%)					
Event	$\delta^{18}O$	$\delta^{2}H$	Ca^{2+}	NO_3^-	SO_4^{2-}	EC
#1	78.17±10.22	59.65±13.87	56.67±1.42	65.45±1.92	65.21±3.20	55.58±2.66
#2	6.72±1.49	15.68±2.84	67.70±1.20	82.84±4.50	83.17±2.95	64.67±2.17
#3	41.99±13.90	42.61±12.33	50.92±0.85	57.08±0.77	57.96±3.84	53.15±2.11
#4	-[a]	68.15±14.48	45.45±0.98	61.99±2.06	63.53±3.28	48.37±2.10
#5	11.79±0.85	20.44±1.30	43.77±0.94	40.35±2.31	51.83±5.03	39.92±2.09
#6	52.06±34.19	30.90±8.05	23.39±1.51	33.24±1.24	32.92±6.13	41.01±2.39
#7	137.17±53.13	63.92±9.22	49.57±1.10	69.19±3.93	64.11±3.24	48.56±2.15
#8	44.35±5.29	28.88±1.83	23.16±1.20	29.26±1.75	33.45±5.89	94.65±6.37[b]

[a] Unrealistic event-water fractions were obtained because the $\delta^{18}O$ signatures in precipitation and streamwater were too similar.

[b] Wash-off of road salt resulted in unrealistic event-water fractions based on EC.